

The Variable Stars of the Draco Dwarf Spheroidal Galaxy - Revisited

K. Kinemuchi

*Departamento de Astronomía, Universidad de Concepción, Concepción, Chile &
Department of Astronomy, University of Florida, Gainesville, Florida, 32611, USA.*

H.C. Harris

US Naval Observatory - Flagstaff Station, Flagstaff, AZ 86001

Horace. A. Smith

Department of Physics & Astronomy, Michigan State University, East Lansing, MI 48824

N. A. Silbermann

Spitzer Science Center, Mail Stop 220-6, Pasadena, CA 91125

L.A. Snyder

Department of Physics & Astronomy, Michigan State University, East Lansing, MI 48824

A. P. LaCluyzé

Department of Physics & Astronomy, Michigan State University, East Lansing, MI 48824

C. L. Clark

Department of Physics & Astronomy, Michigan State University, East Lansing, MI 48824

ABSTRACT

We present a CCD survey of variable stars in the Draco dwarf spheroidal galaxy. This survey, which has the largest areal coverage since the original variable star survey by Baade & Swope, includes photometry for 270 RR Lyrae stars, 9 anomalous Cepheids, 2 eclipsing binaries, and 12 slow, irregular red variables, as well as 30 background QSOs. Twenty-six probable double-mode RR Lyrae stars were identified. Observed parameters, including mean V and I magnitudes, V amplitudes, and periods, have been derived. Photometric metallicities of the ab-type RR Lyrae stars were calculated according to the method of Jurcsik & Kovacs, yielding a mean metallicity of $\langle [Fe/H] \rangle = -2.19 \pm 0.03$. The

well known Oosterhoff intermediate nature of the RR Lyrae stars in Draco is reconfirmed, although the double-mode RR Lyrae stars with one exception have properties similar to those found in Oosterhoff type II globular clusters. The period-luminosity relation of the anomalous Cepheids is rediscussed with the addition of the new Draco anomalous Cepheids.

Subject headings: Variable stars: RR Lyrae, anomalous Cepheids, long period variables — dwarf spheroidal galaxy: Draco

1. Introduction

The Draco dwarf spheroidal (dSph) galaxy ($\alpha_{2000.0} = 17^h 20^m 12.39^s$, $\delta_{2000.0} = +57^\circ 54' 55.3''$), a satellite of the Milky Way Galaxy, was first extensively studied by Baade & Swope (1961) (hereafter known as B&S). They reported discovering over 260 variable stars and obtained photometry for 138 variables in the central region of Draco, 133 of which were of RR Lyrae (RRL) type. Several subsequent studies have investigated aspects of the variable star population in Draco. Zinn & Searle (1976) reported new observations of the anomalous Cepheids in Draco. Nemec (1985a) reanalyzed the B&S photometry and produced updated periods for the B&S variables. Both Nemec (1985a) and Goranskij (1982) reported new double-mode RRL in Draco. Recently Bonanos et al. (2004) provided a photometric study of Draco which produced light curves for 146 RRL stars, four anomalous Cepheids, an SX Phe star, and a field eclipsing binary. In this work, we use CCD observations to update the census of variable stars in Draco. We cover an area slightly larger than the full B&S survey, and we discover new variables with smaller amplitudes than those found by B&S. We provide photometric data, periods, and light curves for over 320 variable stars.

This paper is organized in the following manner: Section 2 describes our data acquisition and data reduction processes. Section 3 covers our analysis techniques. Periods, light curves, and classifications of the variable stars are presented in Section 4. A re-discussion of the Oosterhoff classification of the Draco dwarf spheroidal is presented in Section 5. Conclusions are summarized in section 6.

2. Data Acquisition and Reduction

Our survey of the Draco dSph galaxy was conducted at two telescopes: the 1.0m at the US Naval Observatory in Flagstaff, AZ., and the 2.3m telescope at the Wyoming Infrared Observatory (WIRO), at Mt. Jelm, Wyoming. Combined, the two datasets cover a time

interval of four years (1993-1996). Table 1 contains the Heliocentric Julian dates for when the data were observed.

2.1. USNO observations

Images of Draco were taken with the 1.0 m telescope of the U.S. Naval Observatory in Flagstaff, AZ, during the 1995 and 1996 observing seasons. A Tektronix 2048×2048 CCD was used with a pixel size of 0.68 arcsec, giving a field size of 23.2 arcmin. Four fields were observed, each covering one quadrant of Draco, with 1 arcmin overlap between fields, thus covering approximately a square region of 45 arcmin size centered on Draco. The northeast field position was shifted to the east to avoid the bright star just north of Draco. Therefore the northeast and northwest fields did not overlap, and three variable stars (V5, V10, and V117) were missed in this narrow gap. Figure 1 shows the field placement. This areal coverage is larger than any other study of the variable stars in Draco — it covers about four times more area and more than two times the variable stars than the study by Bonanos et al. (2004), and it provides a useful coverage of about two times more area than that of B&S. The Palomar 200 inch telescope used by B&S allowed discovery of some variable stars up to a distance of 24 arcmin from the center of Draco. However, the degraded image quality in the outer parts of their field prevented them from measuring magnitudes or deriving light curves and periods for most variables beyond an 8 arcmin radius from Draco. This coverage includes all known variable stars in Draco from the B&S study except for two stars they identified, which were found at large distances from the galaxy (one far east, V205, and one far west, V333). Also missing from our study are the three stars that lie in the gap between the northeast and northwest fields near the bright star on the north side of Draco. The first part of Table 2 lists these stars.

The images were taken with a Johnson *V* filter throughout the 1995 and 1996 observing seasons, and with a Cousins *I* filter mostly during the 1996 season. The seeing was typically 2", and the exposure times were 15-30 min depending on the seeing. Exposures were taken switching between quadrants, and alternating filters in 1996, so that each quadrant was observed 1-4 times on a given night with a given filter. An effort was made to minimize alias effects by observing each quadrant over 6-8 hours on several nights, by observing over three weeks during several months, and by observing over the full range of months possible each season. A total of 39-41 *V* images and 19-20 *I* images of each quadrant were taken and are included in the following analysis. DAOPHOT (Stetson 1987) was used to measure all images. A small radial correction for image distortion in the corners of each image was applied for the data taken at USNO.

For the goals of identifying variable stars and measuring accurate magnitudes and light curves, five sources contribute errors to these data. Some stars are crowded or near brighter stars and have erroneous measurements. The CCD has a few defects that produce spurious magnitudes for some stars that occasionally fall on a defect. The CCD is not physically flat, so the high center and low corners produce images of stars in the corners of the field that are not in perfect focus – together with astigmatism, the resulting magnitudes have some additional error. The desire for short exposure times has resulted in images that have typically 0.03 mag error for each observation for the RR Lyr and other horizontal-branch stars in Draco. Finally, the inevitable cosmic rays occasionally affect a star image. Therefore, potential variable stars were examined by eye to decide on real vs. spurious variables. Table 2 also lists those stars that B&S originally marked as variable candidates but which were found not to be variable in our survey. The instrumental magnitudes were shifted onto a common system, iteratively rejecting variable stars, using a method similar to that described by Honeycutt (1992).

Finally the USNO instrumental magnitudes were transformed to standard Johnson V and Cousins I magnitudes as follows. On three photometric nights when Draco images were taken in all quadrants, Landolt (1992) standards were also observed and used to determine transformation coefficients of the form

$$V = v + C_0 + C_1 * (V - I) + C_2 * Airmass \quad (1)$$

and similarly for I . On one additional photometric night, using a different Tektronix 1024x1024 CCD, images were taken centered on Draco, together with Landolt standards. Color coefficients were small, typically 0.01 and 0.03 in V and I , respectively. These coefficients are presented in Table 3 for both V and I bands and per photometric night. Three nights were used to determine mean V and I standard magnitudes for a subset of bright (16-18 mag) nonvariable stars in the Draco images. The transformation of instrumental magnitudes (after shifting onto the common system) to standard magnitudes for this subset of bright stars then was applied to all stars. A comparison of the resulting standard magnitudes for nonvariable stars with Stetson’s Draco calibration region¹ shows good agreement.

The resulting errors in photometry for a single observation are estimated to be 0.01 from calibration uncertainties, 0.02 from image distortion in the CCD corners, and photon noise that increases from 0.01 at $V = 18$ to 0.03 at $V = 20$ to 0.05 at $V = 21$. After combining frames, the errors in the mean magnitudes of nonvariable stars at the level of the horizontal branch ($V = 20$) are estimated to be 0.03 in V , 0.03 in I , and 0.04 in $V - I$. The errors in

¹<http://cadwww.hia.nrc.ca/cadcbn/wdb/astrocat/stetson/query/>

the mean magnitudes of variable stars are generally larger.

2.2. WIRO Observations

The USNO dataset was combined with data obtained at WIRO during the summer quarter observing season of 1993 and 1994. An RCA 337×527 pix CCD camera was used, which had a 1.2 "/pix plate scale. The field of view was much smaller compared to the USNO dataset. The WIRO fields were $6.4 \times 10.4'$ and overlapped with three quadrants of the USNO fields. One WIRO field is roughly 13% of one USNO field. Figure 1 shows where the WIRO fields are in relation to the USNO fields. The data were obtained with Johnson V and Cousins I filters. From WIRO, a maximum of 28 V and 18 I -band images supplemented the USNO data. All available data from WIRO was used for light curve and period analysis of the variable stars. This brings a maximum of 69 V and 38 I images for stars found in both USNO and WIRO fields.

The WIRO observations were placed on a standard system by using secondary standards from the USNO analysis. A total of 45 stars were used for the calibration, and the dominant source of uncertainty are from the original calibration done with the USNO dataset for each bandpass (see section 2.1). Equation 2 and 3 are the transformation equations for the WIRO dataset. The coefficients α_V and α_I were field dependent and were determined from a weighted mean of differences. The coefficients β and γ were obtained from a linear least squares fit between $(V - v_0)$ and $(V - I)$. The standard V magnitude was found through an iterative process, incorporating the standard I magnitude of that star. The values of the transformation coefficients for the WIRO dataset are given in Table 4.

$$V = v_0 - \alpha_V + \beta(v_0 - I) + \gamma \quad (2)$$

$$I = i_0 - \alpha_I \quad (3)$$

Photometry was performed on the WIRO data using Stetson's DAOPHOT II and ALL-FRAME stand alone package (Stetson 1987, 1994).

2.3. Variable Star Identifications

We have kept the original numbering system of B&S for the first 203 variable stars plus number 204 assigned by Zinn & Searle (1976). All new variable star identifications, as

well as the new long period variable stars and the QSOs, are an extension of B&S’s system, but organized by right ascension going east to west. Our new star identification, therefore, begins from V205 through V333.

Stars with high dispersion or high chi-square for their magnitude were considered to be potential variables and inspected further. For the USNO dataset, we used a plot of chi-squared vs. magnitude to identify potential variables. We did not use the Welch & Stetson variability index (Welch & Stetson 1993) because it is defined to make use of pairs of images taken at nearly the same time, and the USNO data generally included unpaired images in each quadrant each night. Image differencing might in retrospect be useful as an additional tool; however, it is more advantageous in fields more crowded than Draco.

For the WIRO dataset, the variable stars were selected by using a simple variability index which compared the external to internal uncertainties of the observations. Our results were then compared to the B&S catalog and we identified the known variable stars. New variables were found and classified by their color, period, and location in the color-magnitude diagram (CMD). Due to the overlap of the WIRO fields with the USNO fields, the variable stars found were checked and confirmed between the two datasets.

A total of 270 RR Lyrae stars, 9 anomalous Cepheids, 12 semi-irregular or carbon stars, and 2 eclipsing binaries were discovered in this survey. We were able to recover all of the original B&S variable stars, and reclassified 7 stars. We discuss the variable stars of Draco in more detail in section 4.

2.4. Comparison with Bonanos et al. (2004)

As discussed in section 2.1, our survey of Draco is nearly four times larger in area and twice the number of variable stars as were found than in Bonanos et al. (2004)’s survey. Because of a match up error in preparing their tables, the periods, magnitudes, and the identifications of 48 stars do not match the RA/DEC star names in Bonanos’ Tables 1 and 2. We have used corrected versions of the tables, kindly provided by A. Bonanos, to make the comparison here. We independently recovered 130 stars that had been found in both the original B&S and Bonanos et al. surveys. Those stars with the B04 designation in our Table 5 have been identified in Bonanos et al. They also identified 17 new RRL stars and one new eclipsing variable; we independently recover all 18 of these stars and make the same classifications, although we find one star (V289) to be an RRd that Bonanos et al. classified as RRab. For this star, we were able to find a period ($P = 0.6607$ days) close to Bonanos et al. period, but it produced a noisy light curve with our data. Our solution produces a

tighter light curve for our photometry. Bonanos et al. identify 9 red variables with small amplitudes near the tip of the giant branch. We find four of them to vary, and find the other five not to vary significantly in our data, so we omit them from our tables. Finally, the SX Phe star Bonanos et al. found was too faint for our survey and was not included in our analysis. For most RRL stars, we find excellent agreement with the periods and RRab/RRc classifications with Bonanos et al. The typical difference between Bonanos et al.’s and our periods for the RRL stars is 0.00002 days. For a few stars, we find a different alias period. The greater number of nights covered by our observations usually make alias problems less important in our analysis, so we prefer our period solutions.

3. Data Analysis

Once the datasets from USNO and WIRO were independently reduced, the data were combined. This increased the number of epochs for 103 variable stars. Using our combined datasets, we present a robust CMD of the Draco dSph galaxy down to a limiting magnitude of $V = 21$ in figure 2. In this updated CMD, we have identified pulsating and eclipsing stars as well as background QSOs in the Draco field. Our census has yielded 279 stars that are either of the RR Lyrae or Cepheid type of pulsating variable star. We have found 12 variable stars which were not RRL, anomalous Cepheids, or eclipsing stars, but belong to other types, either slow, semi-regular, red, or other objects. There appears to be 30 background QSOs found in our coverage of the Draco galaxy. The rest of the stars plotted in figure 2 are non-variable stars (approximately 4700 stars). There is also contamination of field stars from the Milky Way, and thus, a likelihood of field RRL in our survey. We address this possibility in section 4.1. Figure 3 is a close up view of the horizontal branch region of the CMD. Here we identify the individual RRL Bailey types as well as the non-variable stars. We note that there is a large scatter of nearly 0.4 magnitudes for the RRL.

The subsequent analysis was done in four steps: 1) period searching, 2) amplitudes and mean magnitudes calculation, 3) Fourier decomposition of the light curves, and 4) deriving distances from the RRL population. The Fourier decomposition work is discussed in detail in section 4.2.

For the full dataset, we anticipated minimizing any period alias solutions, specifically any yearly aliases. Our primary period searching method was the date compensated discrete Fourier transform (DCDFT) program (Ferraz-Mello 1981; Foster 1995). This program was particularly useful for datasets that have a patchy distribution of data points (i.e. the observations were more or less annual). The actual DCDFT program is part of the CLEANEST program (Foster 1995). An updated version of this program is available through Peranso

². As a check for the period solutions, the IRAF version of the phase dispersion minimization statistic (PDM) (Stellingwerf 1978) was used as well as the Supersmoother routine (Reimann 1994). Overall our periods are good to about 0.00001 to 0.00003 days. To obtain the amplitudes of the V and I variable star data, we use a spline fit to the phased light curve.

4. Variable Star Census

4.1. RR Lyrae Stars

Figure 4 shows the phased V and I light curves. The V light curves have our best spline fit included to aid the eye. Fourier series fits to our light curves were not used because they often give biased results at rapidly changing phases (rising and maximum light) if few data points are available to constrain the fit. With typically 40 V observations, some stars in our data have few points at these phases. Table 5 lists the RRL positions (RA and DEC J2000.0), the period solutions (column 4), the V amplitude (column 5), the intensity-weighted mean magnitudes in V and I (columns 6 and 7), and the type of RRL with additional notes (column 8). We find in our survey 270 RR Lyrae stars, of which 214 are RRab, 30 RRc, and 26 RRd stars. Of these 81 are new RRL compared to the B&S study. Including these new RRL stars, we find the average period of the RRab stars to be $\langle P_{ab} \rangle = 0.615 \pm 0.003$ days and for the RRc stars an average period $\langle P_c \rangle = 0.375 \pm 0.006$ days. In Figure 5, we show the period distribution of the RRL stars. The average period for the RRd stars is $\langle P_d \rangle = 0.407 \pm 0.002$ days. As originally noted by B&S, the mean period of the RRab stars is Oosterhoff intermediate. The Oosterhoff properties of the Draco dwarf system are discussed more fully in section 5.

Foreground RRL have been found in our survey. Using the surface density for RRL in the SA57 field (Kinman et al. 1994), and assuming a halo space density of $R^{-3.5}$, we calculated the volume and RRL per magnitude along our line of sight. From the calculation, we expected 0.9 field RRL in the line of sight, but in actuality we find 3 field RRL (V327, V321, and V276). One of these stars (V327) was previously discovered by Wehlau et al. (1986). The distribution of stars per magnitude peaked around $V = 17$, thus we should see field RRL around this magnitude. The three field RRL are flagged in the main RRL properties table, Table 5.

²www.peranso.com

4.1.1. *Double-Mode RR Lyrae Stars*

Goranskij (1982) used the photometry of Baade & Swope (1961) to identify three RR Lyrae stars in Draco that were pulsating simultaneously in the first overtone and fundamental radial modes. Also using the Baade & Swope (1961) observations, Nemec (1985a) identified seven more of these stars (RRd variables in Nemec’s nomenclature, or RR01 stars in the nomenclature of Clement et al. 2001). Bonanos et al. (2004) redetermined periods for six of the RRd stars found by Nemec (1985a).

We carried out a search for double-mode behavior among the RR Lyrae stars that had light curves that did not seem to be adequately described by a single period. Using the CLEANest routine (Foster 1995) to prewhiten the V-band observations, we removed the primary frequency and its first four harmonics. A search was then undertaken for evidence of a significant secondary period. If a secondary period seemed possible, the CLEANest routine was used to simultaneously fit the primary and secondary periods and their first four harmonics. Although higher order harmonics and cross frequency terms have been detected in the light curves of double-mode RR Lyrae stars, the current set of observations is not sufficient to identify them. For suspected RRd stars, results from the CLEANest routine were verified using the Period04 program (Lenz & Breger 2005).

By this means we found all ten of the RRd stars identified by Goranskij (1982) and Nemec (1985a). In addition, we have identified 16 probable RRd variables, giving a total of 26. The first overtone mode was the dominant mode in each case. First overtone mode periods, fundamental mode periods, and period ratios for probable RRd stars are shown in Table 6. The listed uncertainties are the formal errors given by the CLEANest program. Results for stars with asterisks are more uncertain, usually because of the possibility of a period alias for the fundamental mode period. Deconvolved first overtone and fundamental mode period light curves for the RRd stars are shown in Figure 6.

In plotting the Petersen diagram (Petersen 1973) of period ratio versus fundamental period, Nemec (1985a) discovered that V165 had a position in this diagram similar to those seen among RRd stars in Oosterhoff type I globular clusters, but that all of the other stars had properties similar to those of RRd stars in Oosterhoff type II clusters. Figure 7 shows the Petersen diagram for all 26 probable RRd stars. RRd stars whose locations in this diagram are somewhat uncertain (the asterisked stars in Table 6) are plotted as open points. For comparison, the locations of RRd stars in the Oosterhoff type I globular cluster IC 4499 (Walker & Nemec 1996) and the Oosterhoff type II globular clusters M15 and M68 (Nemec 1985b; Purdue et al. 1995; Walker 1994) are also plotted. V165 still remains the only RRd star with properties similar to those of RRd stars in Oosterhoff type I clusters.

Figure 8 plots the luminosity weighted mean V magnitude against the primary period for all of the Draco RR Lyrae stars. V165, the sole Oosterhoff type I RRd star, is also the faintest RRd star. This is at least qualitatively consistent with other findings that RR Lyrae stars in Oosterhoff type I clusters are less luminous than those in Oosterhoff type II systems (e.g., Sandage 1958; Sandage et al. 1981).

4.1.2. Blazhko Effect

The Blazhko effect is a second order modulation most evident in the shape of the RRL light curve. The maximum light phase can be depressed by the Blazhko effect. This effect is also periodic – on the order of tens to hundreds of days. What causes the Blazhko effect is not clearly known, but there are several proposed explanations (see Kolenberg et al. 2006; Stothers 2006).

We do not have enough observations to determine Blazhko periods for those RRL stars in our sample that show the Blazhko effect. We can, however, identify as Blazhko effect candidates those RRL stars that have unusually large scatter in their light curves and which do not seem to be RRd stars. We list these Blazhko candidates in Table 5 by noting “BI” in the last column. Stars V26, V33, V34, V35, V37, V39, V41, V68, V75, V96, V123, V129, V147, V150, V160, V184, and V196 have already been identified as possible Blazhko variables by Nemec (1985a) and Bonanos et al. (2004). The mean period of the Blazhko effect candidates among the RRab stars is $\langle P_{Bl} \rangle = 0.603 \pm 0.006$ days.

4.2. Fourier Decomposition

The Fourier decomposition of the light curves was done only on the V data. Using Simon’s MINFIT program (Simon 1979; Simon & Teays 1982), a cosine series up to 8th order was fit to the light curves:

$$m = A_0 + \sum A_i \cos(i\omega(t - t_0) + \phi_0) \quad \text{where } i = 1, 2 \dots \quad (4)$$

Once the amplitude (A_i) and phase (ϕ_i) terms were obtained, the Fourier parameters, R_{ji} and ϕ_{ji} , were calculated up to the 4th order.

We applied the Jurcsik & Kovacs (1996) photometric metallicity relation using the Fourier decomposition parameter ϕ_{31} and the period (their equation 3). The Jurcsik & Kovacs method works best when RRab light curves are fully sampled and where photo-

metric uncertainties are relatively small. The light curves for individual RRab stars in our sample do not always meet these criteria. To test the quality of the RRab light curve for this method, a compatibility test called the D_M deviation parameter, is calculated. This deviation parameter is determined from a comparison of the observed and predicted Fourier parameters. An updated version of this test is provided in Kovacs & Kanbur (1998). In order for a star to be a good candidate for the Jurcsik & Kovacs method, the D_M parameter criterion must be met. For our RRab sample, we chose $D_M < 3.0$ (as recommended by Jurcsik & Kovacs) and $D_M < 5.0$ (as recommended by Clement & Shelton 1999). Stars that have passed the criteria are listed in Table 7 with asterisks. Table 7 also lists the Fourier decomposition parameters and photometric metallicities of the Draco RRab stars. All photometric metallicities are on the metallicity scale of the Jurcsik & Kovacs method (Jurcsik 1995).

The $[\text{Fe}/\text{H}]$ values derived from the Jurcsik & Kovacs method may in this case be more useful in deriving a mean $[\text{Fe}/\text{H}]$ value for Draco than in the determination of metallicities for individual stars. It is quite likely that some of the outlying $[\text{Fe}/\text{H}]$ values in Table 7, at both the high and low end do not really reflect the metallicities of the stars for which they are derived. The average $[\text{Fe}/\text{H}]$ for Draco, as determined by the photometric metallicities of the RRab stars, is $\langle [Fe/H] \rangle = -2.19 \pm 0.03$, if we assume the stars are not undergoing the Blazhko effect (see section 4.1.1) and have passed the $D_M < 3.0$ criterion. For the case where $D_M < 5.0$, and assuming no Blazhko, the average metallicity of Draco is $\langle [Fe/H] \rangle = -2.23 \pm 0.03$. Figure 9 shows the metallicity distribution of the RRab stars that have passed the $D_M < 5.0$ criterion with respect to period.

Using Stromgren photometry, Faria et al. (2007) recently obtained a mean $[Fe/H]$ of -1.74 for Draco and field red giant branch stars, with most stars falling within the limits $-1.5 > [Fe/H] > -2.0$. That result is broadly consistent with the earlier results of Shetrone et al. (2001b) and Zinn (1978), although Shetrone et al. did find one red giant star as metal poor as $[Fe/H] = -2.97$. Faria et al. (2007) calibrated their derived metallicities to the work of Hilker (2000), which analyzed the red giants of three globular clusters and spanned a metallicity range of -2.0 to 0.0 dex. Therefore, we must be cautious when comparing our metallicity results to those of other studies since there are dependencies to various metallicity calibrations. However, there is a suggestion that the average metallicity of the Draco RRab stars is lower than that of the Draco red giant stars. The reality of this difference in metallicity is uncertain due to the nature of the different calibration methods. If this difference is real, then presumably the red horizontal branch stars in Draco would have to be more metal-rich on average than the RRab stars.

4.3. RRL distance for Draco

Since RRL are excellent distance indicators, we calculate the distance to the Draco dwarf galaxy. We use the metal-poor ($[Fe/H] < 1.5$) relation from Cacciari & Clementini (2003) (their equation 4). As with Bonanos et al.’s work, we use an $E(B - V) = 0.027$ from the Schlegel et al. (1998) reddening maps, and the corrections for the extinction as suggested by the work of Cardelli et al. (1989), thus, $A_V = 0.091$. From our sample of RRL stars, the intensity-weighted mean V magnitude is $\langle V \rangle = 20.10 \pm 0.04$ ($\sigma_{RMS} = 0.08$). For this value, we omitted the magnitudes of the foreground RRL (V276, V321, and V327) and V176 since it is blended with a bright star. The uncertainties given for this mean magnitude accounts for the calibration errors, image distortion, and photon noise (see Section 2.1). The value of $\langle V(RR) \rangle = 20.10 \pm 0.04$ in this paper is brighter than those of Bonanos et al. (2004): $\langle V(RR) \rangle = 20.18 \pm 0.02$, of Aparicio et al. (2001): $\langle V(HB) \rangle = 20.2 \pm 0.1$, and of Bellazzini et al. (2002): $\langle V(HB) \rangle = 20.28 \pm 0.10$, with a 2-sigma difference from the most precise value of Bonanos et al.

If we assume a metallicity for Draco from our Fourier decomposition analysis, $[Fe/H] = -2.19 \pm 0.03$, and using the Cacciari & Clementini (2003) relation, our resultant absolute magnitude is $\langle M_V \rangle = 0.43 \pm 0.13$. Therefore, using the present mean V magnitude of the RRL stars and accounting for the extinction, we derive a dereddened distance modulus to Draco of $\mu_0 = 19.58$ or $D = 82.4 \pm 5.8$ kpc. However, if we assume a different metallicity for Draco, our distance changes slightly. Shetrone et al. (2001b) obtained a mean metallicity of $[Fe/H] = -2.00 \pm 0.21$ from high resolution spectroscopy of Draco red giants, whereas Faria et al. (2007) found $[Fe/H] = -1.74$. If we assume the metallicity values of -2.00 and -1.74 , and using the same Cacciari & Clementini relation and the present RRL mean V magnitude, the resultant distances are 81.2 and 79.8 kpc, respectively. Pritzl et al. (2002a) arrived at a distance to Draco independently from the anomalous Cepheid stars (see section 4.4). Their value is $\mu_0 = 19.49$ or $D = 79.1$ kpc, but using a reddening value of $E(B - V) = 0.03$. Within our uncertainties, we agree with all these distance values from different Draco studies.

4.4. Anomalous Cepheids

In our study of the Draco dwarf galaxy, we increase the number of known anomalous Cepheids (AC) to nine. Baade & Swope (1961) had identified what appeared to be five overly bright RR Lyrae stars in their original survey. Norris & Zinn (1975), followed by Zinn & Searle (1976) first classified these variables as AC stars (V134, V141, V157, V194, and V204). Nemec et al. (1988a) reidentified the five stars in Draco as AC, based on a

reanalysis of B&S’s photographic survey. These five AC stars were confirmed in our study. We have been able to add four new AC’s: V31, V230, V282, and V312, to the census. Table 8 lists all the photometrically derived parameters.

Of the new anomalous Cepheids, one star, V31, has been reclassified. Originally, it was identified by B&S as an RRL variable star based on eye estimates only. However, it lies only 13” from a bright BD star. The I and the $V - I$ color are particularly uncertain because of scattered light from the nearby bright red star. Our CCD data show that it is significantly brighter than other Draco RRL stars, so we believe it is a new AC. The bright star is saturated in our data and contributes significant scattered light around V31. Nevertheless, after doing careful background subtraction, the estimated errors in our photometry are 0.1 in V and 0.2 in I , leaving it 0.5 mag brighter than the horizontal branch. The other AC stars do not have companions visible in our data. Furthermore, most are either sufficiently bright or have large amplitudes that they cannot be an RRL star made brighter by an unresolved companion. However for V31, V230, and V282, we cannot exclude this possibility of RRL-plus-unresolved companion. In Figure 10 we present the light curves of all the AC found in this survey with a spline fit added to aid the eye.

Generally, these variable stars are brighter than the RRL population by 0.5 (for shorter period, $P \sim 0.3$ days) to 2 magnitudes (longer period, $P \sim 2.0$ days). These stars are also more massive than the RRL, typically 1.0-2.0 M_{\odot} (Pritzl et al. 2002a, and references therein), and must be relatively metal-poor in order for the progenitor stars to reach the instability strip. Anomalous Cepheids have been found in all the known dwarf spheroidal galaxies of the Local Group, however, they are not typically found in the Galactic globular clusters. The exceptions are V19 in NGC 5466 (Zinn & Dahn 1976) and two candidates in ω Cen (Wallerstein & Cox 1984). XZ Ceti is a well known field AC. The origins of these stars still remains unsolved, but the leading theories suggest that they are either 1) intermediate aged stars ($t < 5$ Gyrs) or 2) primordial binary systems undergoing mass transfer. These mechanisms provide alternative origins for the blue straggler populations that have been speculated to be the progenitor stars of the AC.

Recently, Momany et al. (2007) investigated the frequency of blue straggler stars in the Local Group dSph population, compared to the frequency of such stars in Galactic globular clusters, open clusters, and the field. They find that, in general, the blue straggler frequency is higher in dSph galaxies than in globular clusters. If the blue straggler stars are progenitors of the ACs, then this higher frequency is consistent with a higher frequency of ACs among the dSph systems. It is noteworthy, too, that some mechanisms for creating blue stragglers by mass transfer may not operate in systems of low stellar density, such as the dSph. For example it has been suggested that collisional binary systems might create blue straggler

stars, but such collisions would be infrequent in dSph systems (Momany et al. 2007). Thus, to consider the blue straggler star frequency, one must only consider those stellar formation mechanisms that will be likely in a dSph environment if one wishes to correlate with the number of AC stars found.

Anomalous Cepheids of dSph galaxies have also been used to create a period-luminosity (P-L) relation. Recent work by Dall’Ora et al. (2003), Pritzl et al. (2002a), and Nemec et al. (1994) have presented empirical anomalous Cepheid P-L relations associated with the pulsational mode. Both empirical and theoretical P-L relations have shown that they are not parallel (Pritzl et al. 2002a; Bono et al. 1997). However, there is still some question as to whether the two apparent P-L relations are real, due to distinct fundamental and first-overtone mode relations, or whether the results might instead be interpreted as a single P-L relation with large scatter. That scatter might be a reflection of the range of AC masses as well as the finite width of the instability strip.

For the Draco AC sample, we applied the empirical P-L relations of Pritzl et al. (2002a) to see whether the location of the additional Draco stars would support the reality of two distinct P-L relations. We have calculated absolute magnitudes for the Draco AC stars assuming a distance modulus of $(m - M)_0 = 19.49$ and an $E(B - V) = 0.03$ (Pritzl et al. 2002a) in order to incorporate our results with their empirical P-L relations. Figure 11 shows the location of the Draco AC stars with respect to the AC stars found in other Local Group dwarf galaxies. We see that most of the Draco ACs (V31, V141, V157, V194, V230, V282, and V312) fall along the P-L relation for stars pulsating in the fundamental mode, but two, V134 and V204, fall closer to the first overtone mode P-L relation. As discussed in Pritzl et al. (2002a), it is difficult to assign the pulsational mode in this manner, especially if phase coverage is not complete. We find that to be the case for the Draco ACs as well. Two possible first overtone pulsators, V134 and V204, have light curves showing only modest asymmetry. Among RR Lyrae stars that is a sign of RRc or first overtone mode pulsation. However, the light curves for the supposed fundamental mode pulsator, V194, seems similar. Thus, we can only indicate that while there is evidence in Figure 11 for two distinct AC P-L relations, the actual situation is still uncertain. For example, a range of masses among the ACs might influence the positions of the Draco AC within the P-L diagram, and it perhaps cannot be entirely excluded that a single P-L relation with scatter could account for the observations.

4.5. Other Variable Stars

Three categories of variable stars other than RR Lyraes and Cepheids appear in our data: two eclipsing binaries, 30 “bluish long-period variables”, 12 red semi-regular or irregular variables, and carbon stars have been found and are listed in Tables 9 and 10. The following subsections discuss each of these types of stars.

4.5.1. Eclipsing Binary Stars

A field eclipsing binary star (V296) was found in the survey completed by Bonanos et al. (2004), which we have recovered in our work. We agree with their period solution for this star with a period of 0.2435 days. Figure 12 shows the light curve of V296 phased to this period. Additionally, we have also found another possible eclipsing binary star with a small amplitude change. This star, V256, has few faint observations, and our period result is somewhat uncertain. In Table 9, we provide two plausible period solutions. However, to truly confirm the nature of this eclipsing binary, a careful follow up will be needed to arrive at the correct period.

4.5.2. Carbon Stars

A population of stars redward of the red giant branch (RGB) have been often identified as carbon stars (Aaronson et al. 1983). There are six carbon stars known in Draco (C1-C3 Aaronson et al. 1982); (C4 Azzopardi et al. 1986); (C5 Armandroff et al. 1995); (C6 Shetrone et al. 2001a). We find the stars C1, C2, and C5 to be variable with V amplitudes close to 0.2 mag. Stars C3, C4, and C6 do not appear to vary during two seasons of observations at USNO. Shetrone et al. also reported C2 as a definite variable, and C5 as a possible variable.

The unusual nature of star C1 was noted by Aaronson et al. (1982) and by Margon et al. (2002) from their independent study of the star in a spectrum from the Sloan Digital Sky Survey. The strong emission lines of hydrogen and helium, the blue continuum flux, and the X-ray emission indicate it is a symbiotic carbon star like UV Aur. Therefore, its photometric variability is not surprising. It also has a variable radial velocity (Olszewski et al. 1995) that is likely caused by orbital motion and may be independent of its variable brightness. The other carbon stars, including the two that we find to be variable, have not shown variable velocities.

4.5.3. Long Period Variables and QSOs

The characteristics of the bluish long-period variables are slow variability, no apparent period, amplitudes typically 0.25 mag, colors blueward of the Draco giant branch, and no clear concentration toward Draco. These characteristics suggest that most of them are background QSOs, and this hypothesis has been supported by available spectroscopy. The red semi-regular variables have colors and magnitudes placing them near the tip of the red giant branch (RGB) in Draco, and they all have radial velocities and/or proper motions showing they are members of Draco. Figure 13 shows our time series photometric data of the red long period variable stars. Spline fits were not included since we assume the coverage of the full variation was not obtained through the time coverage of our dataset. Also, due to the approximately 40 V observations, we cannot provide robust estimations in the amplitudes of these long period variables. In Table 9 we list mean magnitudes rather than intensity-weighted mean magnitudes due to our spotty phase coverage and to the low amplitudes of these objects.

B&S remarked on the lack of red variables found in Draco. Bonanos et al. (2004) showed there are variables among the stars near the tip of the giant branch, as is also shown in Figure 2. Our 12 red variables are mostly of low amplitude, and the amplitudes must have been just below the threshold for detection by B&S. We now know that in metal-poor systems like Draco, high-amplitude red variables like Miras are absent, and low amplitude semi-regular or irregular variables are more common (e.g. Harris 1987).

Distinguishing between background QSOs and red variables in Draco is not always obvious, however, because QSOs sometimes can be red, and some Draco variables might be bluish and without regular periods. For example, UU Her and RV Tauri stars are found in globular clusters and could be confused here with our limited data. Therefore, spectroscopy is useful to insure accurate classification: 22 bluish long-period variables are confirmed as QSOs with spectra taken with the WIYN telescope and described in a separate paper (Harris & Munn 2008, in preparation) and/or spectra from the Sloan Digital Sky Survey that put them in the SDSS DR3 QSO Catalog (Schneider et al. 2005). Eight additional variables with similar characteristics are listed in Table 10 as probable QSOs.

The prototype of the QSOs behind Draco, V203, was found by B&S and given in their Table VII, and the light curve spanning over six years was shown in their Fig. 8. They did not understand its nature, but their light curve was the best study of variability of a QSO at that time. Of course, the redshift of QSOs and their characteristic variability was not discovered for two more years (Schmidt 1963; Matthews & Sandage 1963).

5. Draco and the Oosterhoff dichotomy

Oosterhoff (1939) found that five RR Lyrae-rich globular clusters could be divided into two groups, now known as Oosterhoff groups, on the basis of the properties of their RR Lyrae stars. Subsequent investigations found that almost all of the Milky Way globular clusters that contain significant numbers of RR Lyrae stars could be placed into one or the other of the Oosterhoff groups. The RRL in Oosterhoff group I clusters have $\langle P_{ab} \rangle \sim 0.55^d$ and $\langle P_c \rangle \sim 0.32^d$. RRL in Oosterhoff II clusters have $\langle P_{ab} \rangle \sim 0.64^d$ and $\langle P_c \rangle \sim 0.37^d$. Oosterhoff II clusters are also relatively richer in RRc variables than Oosterhoff I clusters, and they are more metal-poor than Oosterhoff I clusters (see, for example Smith 1995). However, not all systems show the Oosterhoff dichotomy. In contrast to the Milky Way globular clusters, dwarf spheroidal systems often have Oosterhoff intermediate properties (for recent discussions, see Pritzl et al. 2002a; Catelan 2004, 2005).

The mean period of RRab stars in Draco found here, 0.615^d , seems to confirm its Oosterhoff intermediate nature. However, a detailed inspection of the the properties of its RRL suggests a complicated picture. The Draco period-amplitude (Bailey) diagram (Figure 14) is consistent with an Oosterhoff intermediate classification. Many of the RRab stars occupy positions in this diagram close to that of the Clement et al. (2001) Oosterhoff I line, but many also fall to the right of that line, in the Oosterhoff intermediate zone. This result is qualitatively true if the trend lines of Cacciari et al. (2005) are used instead of those of Clement & Rowe (2000). The Cacciari et al. (2005) lines are based on the period-amplitude distribution of RRab, some of which are evolved along the horizontal branch, of M3. In the Milky Way, a metallicity of $[Fe/H] = -2.1$ would be typical of globular clusters of Oosterhoff type II. However, the ratio of RRcd to RRab stars in Draco, 0.26, is typical of Oosterhoff type I clusters. In contrast, the RRcd stars in Draco appear dominated by stars having Oosterhoff type II characteristics. This is particularly true of the RRd stars – all but one of which fall in the Petersen diagram in the region occupied by double-mode stars observed in Oosterhoff II clusters such as M15. In summary, RRab stars in the period-amplitude diagram and the mean RRab period suggest an Oosterhoff intermediate class. However, the RRcd population has attributes usually associated with an Oosterhoff type II system. The mean period of the RRcd stars, 0.39 days, is long and the location of the RRd stars in the Petersen diagram suggests a mainly Oosterhoff II class. Figure 5 shows a sharp fall off in the number of RRcd stars as one goes to shorter periods. This in part reflects an overall falloff in the number of HB stars as one goes from red to blue across the instability strip. There is a hint of a bimodal distribution in the RRc periods, but its significance is uncertain because of the small number of RRc stars toward the short period end of the distribution. Conclusions as to the Oosterhoff classification of the RRL stars are probably surer when based upon the more numerous RRab variable stars.

It is plausible that the discordant Oosterhoff properties of the Draco RRL are in some way related to the overall distribution of stars across its horizontal branch. Draco has a HB redder than found among ordinary Oosterhoff II clusters, or among Milky Way globular clusters having $[Fe/H] = -2$ (see for example Catelan 2005). It has been proposed (Lee et al. 1990; Clement & Shelton 1999; Clement et al. 2001) that many RRL in Oosterhoff type II systems have evolved into the blue part of the instability strip from ZAHB positions. The paucity of blue HB stars in Draco makes it unlikely that the majority of its RRL have evolved from ZAHB positions on the blue HB, and thus perhaps it is not surprising that Draco is not an Oosterhoff type II system despite having a low value of $[Fe/H]$. There may, however, be problems with the hypothesis that Oosterhoff II RRL are evolved blue HB stars. Even in the cases of ordinary Oosterhoff type II globular clusters, it has been argued that, according to conventional stellar evolutionary theory, the HB stars evolving from the blue HB would not spend sufficient time in the instability strip to produce the observed numbers of RRL (Renzini & Fusi Pecci 1988; Rood & Crocker 1989; Pritzl et al. 2002b). Thus, the exact role played by Draco’s redder HB in producing its confusing Oosterhoff properties remains uncertain.

According to the Λ -cold dark matter hierarchical model, the outer halo has been assembled partly due to the accretion of objects like the Local Group dwarf galaxy population. However, almost no globular clusters of the Galaxy have Oosterhoff intermediate properties. Nor does the field RRL population of the halo resemble that of Draco (see, for example Kinemuchi et al. 2006). Thus, it seems likely that systems exactly like Draco cannot have been a main contributor to building the halo. In addition, Shetrone et al. (2001a) and Pritzl et al. (2005) found that the patterns of elemental abundances in the dwarf spheroidal galaxies were distinct from those in globular clusters and halo field stars. However, Bellazzini et al. (2002) argue that objects like Draco could still be considered as a building block if we consider that the accretion may have occurred early in the star formation history of the dwarf galaxy or during an early episode of gas stripping by the Galaxy. Our findings with Draco at least imply that objects like this dwarf galaxy could not have contributed to the formation of the outer halo, even if it was accreted before the old population was formed in the dSph galaxy.

6. Summary

We have presented the latest census of variable stars of the Draco dwarf spheroidal galaxy. We have found 81 new RRab stars, 8 new RRC stars, and 16 probable new RRd stars, thus bringing to 214 RRab, 30 RRC and 26 RRd the total number of RRL stars of

the different types known in Draco. We have increased the number of anomalous Cepheids to nine from five. Draco cannot be clearly classified as an Oo I or an Oo II type system. Based upon the mean period of its RRab stars and their location in the period-amplitude diagram, Draco is Oosterhoff intermediate. Objects exactly like Draco are thus not likely to be important building blocks in forming the Galactic halo. We note, however, that the properties of the RRd stars in Draco are, with a single exception, similar to those of RRd stars in Oo II clusters.

The anomalous Cepheids in the Draco dSph galaxy show a possible dual P-L relation stemming from the pulsational modes of the stars. However, with so few stars populating the first-overtone relation, we cannot say with certainty that two P-L relation alternative is the only one capable of describing the relationships of luminosity and period for Draco AC stars. In addition to the pulsating variable stars, we find two field eclipsing binary stars, 30 background QSOs, and 12 long period variable stars.

This research used the facilities of the Canadian Astronomy Data Centre operated by the National Research Council of Canada with the support of the Canadian Space Agency. The identification of QSOs is based partly on spectra obtained with the Hydra multifiber spectrograph on the WIYN telescope at Kitt Peak National Observatory, National Optical Astronomical Observatories. NOAO is operated by the Association of Universities for Research in Astronomy, Inc., under cooperative agreement with the National Science Foundation. This research has made use of the USNOFS Image and Catalogue Archive operated by the United States Naval Observatory, Flagstaff Station (<http://www.nofs.navy.mil/data/fchpix/>).

H.A.S. acknowledges support from NSF grant AST 0607249. K.K. acknowledges support from NSF grant AST-0307778. The authors would like to thank the referee, Gisella Clementini, for very useful comments and detailed suggestions for the overall improvement of this paper.

REFERENCES

- Aaronson, M., Hodge, P. W., & Olszewski, E. W. 1983, *ApJ*, 267, 271
- Aaronson, M., Liebert, J., & Stocke, J. 1982, *ApJ*, 254, 507
- Aparicio, A., Carrera, R., & Martínez-Delgado, D. 2001, *AJ*, 122, 2524
- Armandroff, T. E., Olszewski, E. W., & Pryor, C. 1995, *AJ*, 110, 2131
- Azzopardi, M., Lequeux, J., & Westerlund, B. E. 1986, *A&A*, 161, 232

- Baade, W., & Swope, H. H. 1961, *AJ*, 66, 300
- Bellazzini, M., Ferraro, F. R., Origlia, L., Pancino, E., Monaco, L., & Oliva, E. 2002, *AJ*, 124, 3222
- Bonanos, A. Z., Stanek, K. Z., Szentgyorgyi, A. H., Sasselov, D. D., & Bakos, G. Á. 2004, *AJ*, 127, 861
- Bono, G., Caputo, F., Santolamazza, P., Cassisi, S., & Piersimoni, A. 1997, *AJ*, 113, 2209+
- Cacciari, C., & Clementini, G. 2003, in *Lecture Notes in Physics*, Berlin Springer Verlag, Vol. 635, *Stellar Candles for the Extragalactic Distance Scale*, ed. D. Alloin & W. Gieren, 105–122
- Cacciari, C., Corwin, T. M., & Carney, B. W. 2005, *AJ*, 129, 267
- Cardelli, J. A., Clayton, G. C., & Mathis, J. S. 1989, *ApJ*, 345, 245
- Catelan, M. 2004, in *Astronomical Society of the Pacific Conference Series*, 113–+
- Catelan, M. 2005, *ArXiv Astrophysics e-prints*
- Clement, C. M., Muzzin, A., Dufton, Q., Ponnampalam, T., Wang, J., Burford, J., Richardson, A., Rosebery, T., Rowe, J., & Hogg, H. S. 2001, *AJ*, 122, 2587
- Clement, C. M., & Rowe, J. 2000, *AJ*, 120, 2579
- Clement, C. M., & Shelton, I. 1999, *ApJ*, 515, L85
- Dall’Ora, M., Ripepi, V., Caputo, F., Castellani, V., Bono, G., Smith, H. A., Brocato, E., Buonanno, R., Castellani, M., Corsi, C. E., Marconi, M., Monelli, M., Nonino, M., Pulone, L., & Walker, A. R. 2003, *AJ*, 126, 197
- Faria, D., Feltzing, S., Lundström, I., Gilmore, G., Wahlgren, G. M., Ardeberg, A., & Linde, P. 2007, *A&A*, 465, 357
- Ferraz-Mello, S. 1981, *AJ*, 86, 619+
- Foster, G. 1995, *AJ*, 109, 1889
- Goranskij, V. P. 1982, *Astronomicheskij Tsirkulyar*, 1216, 5+
- Harris, H. C. 1987, in *LNP Vol. 274: Stellar Pulsation*, ed. A. N. Cox, W. M. Sparks, & S. G. Starrfield, 274–283

- Hilker, M. 2000, *A&A*, 355, 994
- Honeycutt, R. K. 1992, *PASP*, 104, 435
- Jurcsik, J. 1995, *Acta Astronomica*, 45, 653
- Jurcsik, J., & Kovacs, G. 1996, *A&A*, 312, 111
- Kinemuchi, K., Smith, H. A., Woźniak, P. R., & McKay, T. A. 2006, *AJ*, 132, 1202
- Kinman, T. D., Suntzeff, N. B., & Kraft, R. P. 1994, *AJ*, 108, 1722
- Kolenberg, K., Smith, H. A., Gazeas, K. D., Elmash, A., Breger, M., Guggenberger, E., van Cauteren, P., Lampens, P., Reegen, P., Niarchos, P. G., Albayrak, B., Selam, S. O., Özavcı, I., & Aksu, O. 2006, *A&A*, 459, 577
- Kovacs, G., & Kanbur, S. M. 1998, *MNRAS*, 295, 834
- Landolt, A. U. 1992, *AJ*, 104, 340
- Lee, Y., Demarque, P., & Zinn, R. 1990, *ApJ*, 350, 155
- Lenz, P., & Breger, M. 2005, *Communications in Asteroseismology*, 146, 53
- Margon, B., Anderson, S. F., Harris, H. C., Strauss, M. A., Knapp, G. R., Fan, X., Schneider, D. P., Vanden Berk, D. E., Schlegel, D. J., Deutsch, E. W., Ivezić, Ž., Hall, P. B., Williams, B. F., Davidsen, A. F., Brinkmann, J., Csabai, I., Hayes, J. J. E., Hennessy, G., Kinney, E. K., Kleinman, S. J., Lamb, D. Q., Long, D., Neilsen, E. H., Nichol, R., Nitta, A., Snedden, S. A., & York, D. G. 2002, *AJ*, 124, 1651
- Matthews, T. A., & Sandage, A. R. 1963, *ApJ*, 138, 30
- Momany, Y., Held, E. V., Saviane, I., Zaggia, S., Rizzi, L., & Gullieuszik, M. 2007, *A&A*, 468, 973
- Nemec, J., Mendes de Oliveira, C., & Wehlau, A. 1988a, in *ASP Conf. Ser. 4: The Extragalactic Distance Scale*, 180+
- Nemec, J. M. 1985a, *AJ*, 90, 204
- . 1985b, *AJ*, 90, 240
- Nemec, J. M., Nemec, A. F. L., & Lutz, T. E. 1994, *AJ*, 108, 222
- Norris, J., & Zinn, R. 1975, *ApJ*, 202, 335

- Olszewski, E. W., Aaronson, M., & Hill, J. M. 1995, *AJ*, 110, 2120
- Oosterhoff, P. T. 1939, *The Observatory*, 62, 104
- Petersen, J. O. 1973, *A&A*, 27, 89
- Pritzl, B. J., Armandroff, T. E., Jacoby, G. H., & Da Costa, G. S. 2002a, *AJ*, 124, 1464
- Pritzl, B. J., Smith, H. A., Catelan, M., & Sweigart, A. V. 2002b, *AJ*, 124, 949
- Pritzl, B. J., Venn, K. A., & Irwin, M. 2005, *AJ*, 130, 2140
- Purdue, P., Silbermann, N. A., Gay, P., & Smith, H. A. 1995, *AJ*, 110, 1712
- Reimann, J. D. 1994, Ph.D. Thesis
- Renzini, A., & Fusi Pecci, F. 1988, *ARA&A*, 26, 199
- Rood, R. T., & Crocker, D. A. 1989, in *IAU Colloq. 111: The Use of pulsating stars in fundamental problems of astronomy*, ed. E. G. Schmidt, 103–119
- Sandage, A. 1958, *Ricerche Astronomiche*, 5, 41
- Sandage, A., Katem, B., & Sandage, M. 1981, *ApJS*, 46, 41
- Schlegel, D. J., Finkbeiner, D. P., & Davis, M. 1998, *ApJ*, 500, 525
- Schmidt, M. 1963, *Nature*, 197, 1040
- Schneider, D. P., Hall, P. B., Richards, G. T., Vanden Berk, D. E., Anderson, S. F., Fan, X., Jester, S., Stoughton, C., Strauss, M. A., SubbaRao, M., Brandt, W. N., Gunn, J. E., Yanny, B., Bahcall, N. A., Barentine, J. C., Blanton, M. R., Boroski, W. N., Brewington, H. J., Brinkmann, J., Brunner, R., Csabai, I., Doi, M., Eisenstein, D. J., Frieman, J. A., Fukugita, M., Gray, J., Harvanek, M., Heckman, T. M., Ivezić, Ž., Kent, S., Kleinman, S. J., Knapp, G. R., Kron, R. G., Krzesinski, J., Long, D. C., Loveday, J., Lupton, R. H., Margon, B., Munn, J. A., Neilsen, E. H., Newberg, H. J., Newman, P. R., Nichol, R. C., Nitta, A., Pier, J. R., Rockosi, C. M., Saxe, D. H., Schlegel, D. J., Snedden, S. A., Szalay, A. S., Thakar, A. R., Uomoto, A., Voges, W., & York, D. G. 2005, *AJ*, 130, 367
- Shetrone, M. D., Côté, P., & Sargent, W. L. W. 2001b, *ApJ*, 548, 592
- Shetrone, M. D., Côté, P., & Stetson, P. B. 2001a, *PASP*, 113, 1122
- Simon, N. R. 1979, *A&A*, 74, 30

- Simon, N. R., & Teays, T. J. 1982, *ApJ*, 261, 586
- Smith, H. A. 1995, *RR Lyrae stars* (Cambridge Astrophysics Series, Cambridge, New York: Cambridge University Press, —c1995)
- Stellingwerf, R. F. 1978, *ApJ*, 224, 953
- Stetson, P. B. 1980, *AJ*, 85, 387
- . 1987, *PASP*, 99, 191
- . 1994, *PASP*, 106, 250
- Stothers, R. B. 2006, *ApJ*, 652, 643
- Walker, A. R. 1994, *AJ*, 108, 555
- Walker, A. R., & Nemeč, J. M. 1996, *AJ*, 112, 2026
- Wallerstein, G., & Cox, A. N. 1984, *PASP*, 96, 677
- Wehlau, A., Bohlender, D., & Demers, S. 1986, *PASP*, 98, 872
- Welch, D. L., & Stetson, P. B. 1993, *AJ*, 105, 1813
- Zinn, R. 1978, *ApJ*, 225, 790
- Zinn, R., & Dahn, C. C. 1976, *AJ*, 81, 527
- Zinn, R., & Searle, L. 1976, *ApJ*, 209, 734

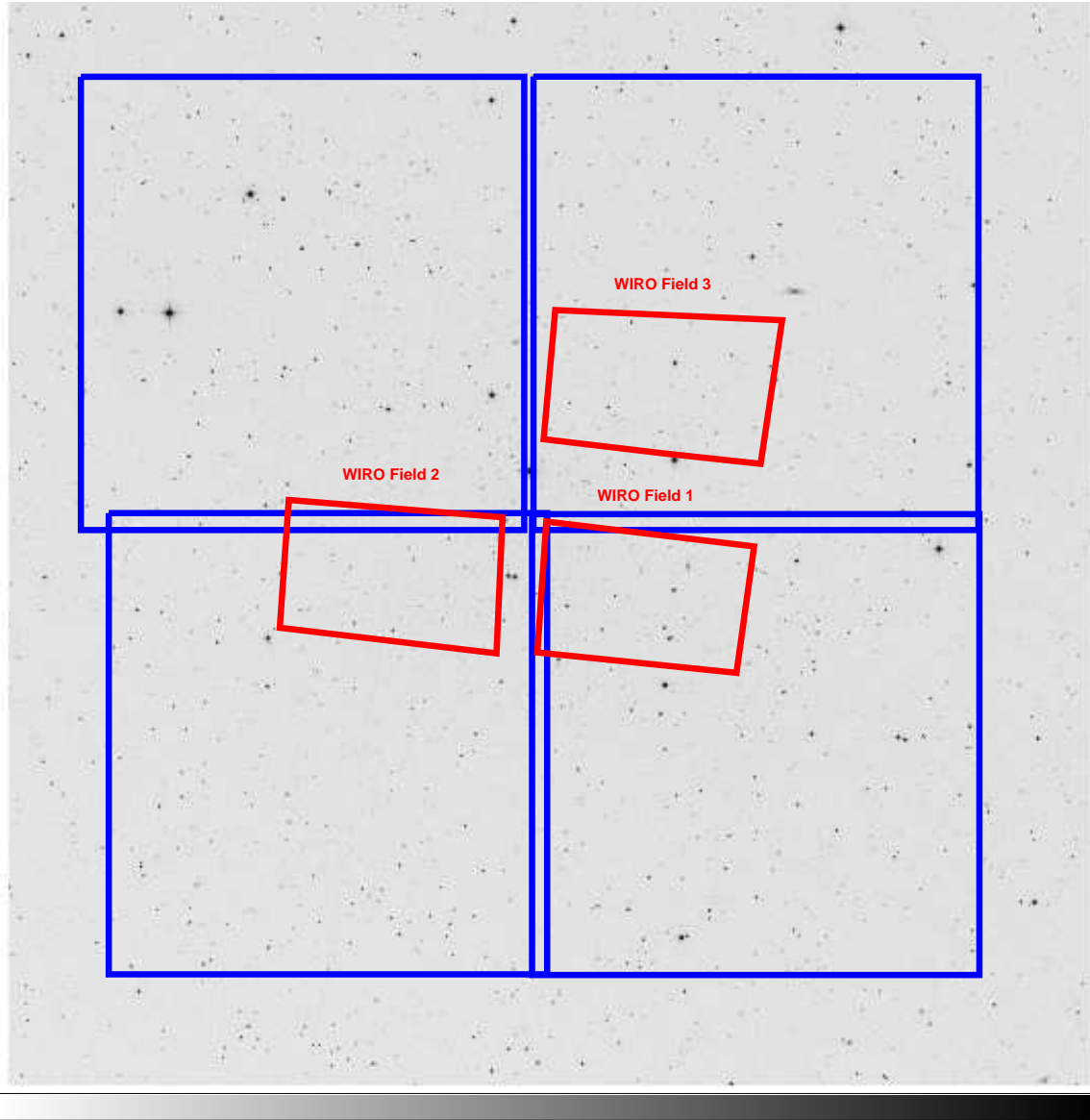


Fig. 1.— The observed fields of the Draco dwarf spheroidal galaxy. The regions outlined in blue are fields observed at USNO while the red boxes are the fields observed at WIRO.

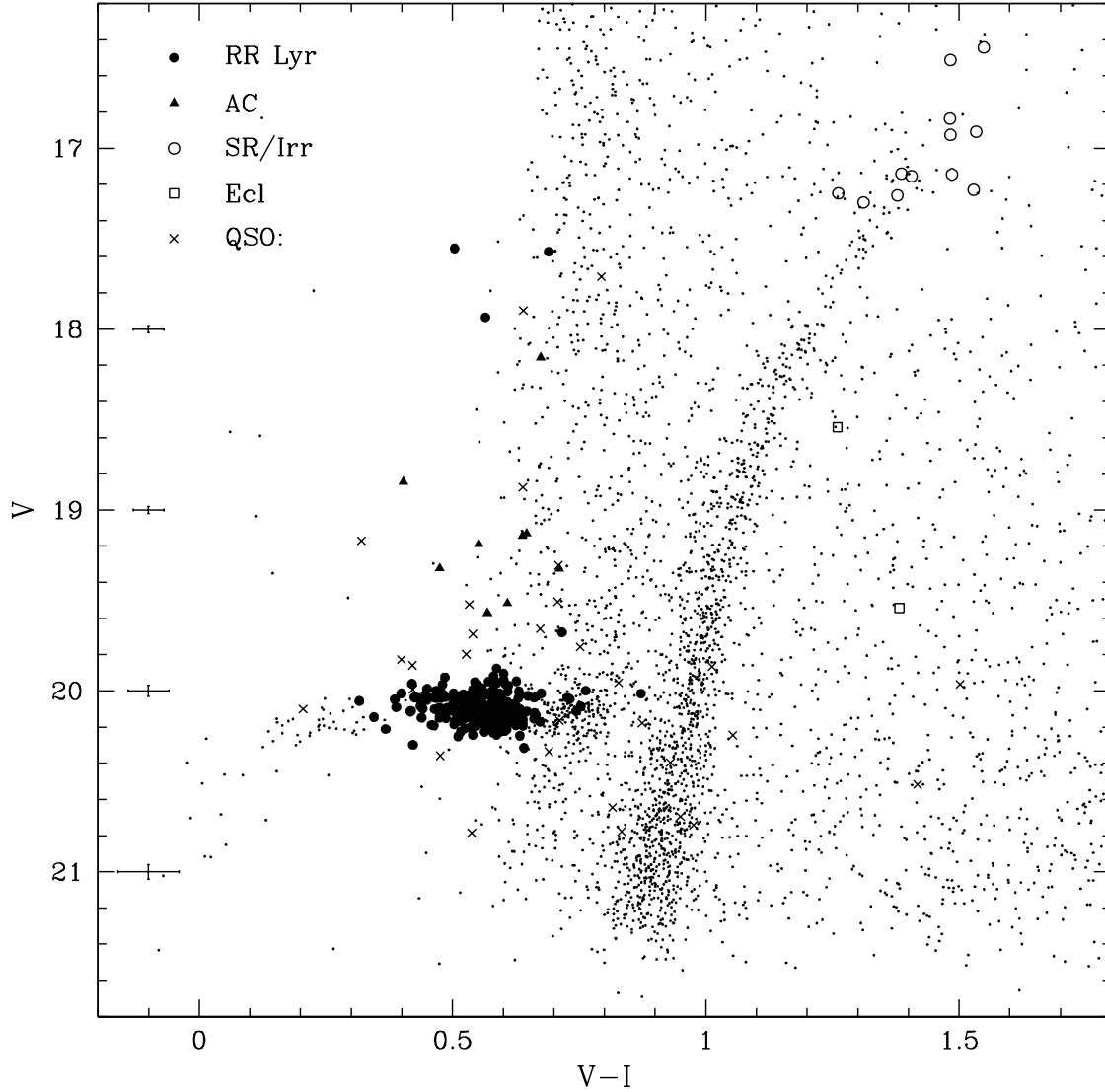


Fig. 2.— Color-magnitude diagram of the Draco dwarf spheroidal galaxy. Variable stars (RR Lyrae, Cepheids, eclipsing binaries, and semi-regular) are identified in the figure. Background QSOs are included in this diagram. Representative error bars for nonvariable stars are shown at the left edge of the figure.

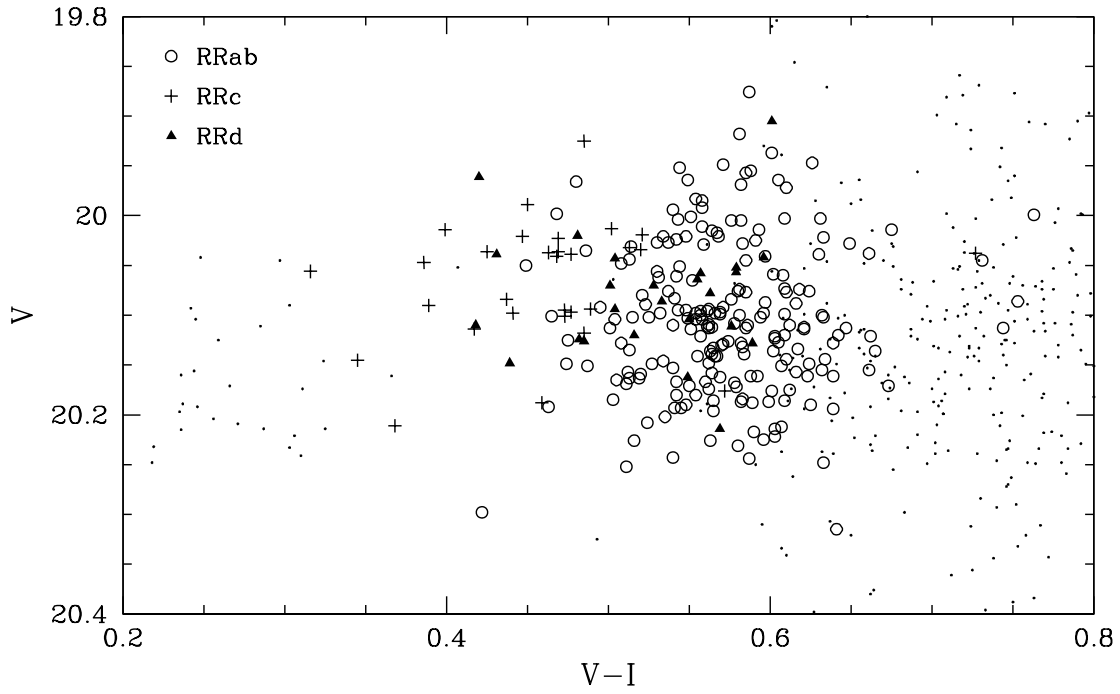


Fig. 3.— A closer view of the horizontal branch. RRab stars are the open circles, RRc stars are the plus signs, and the RRd stars are the filled triangles.

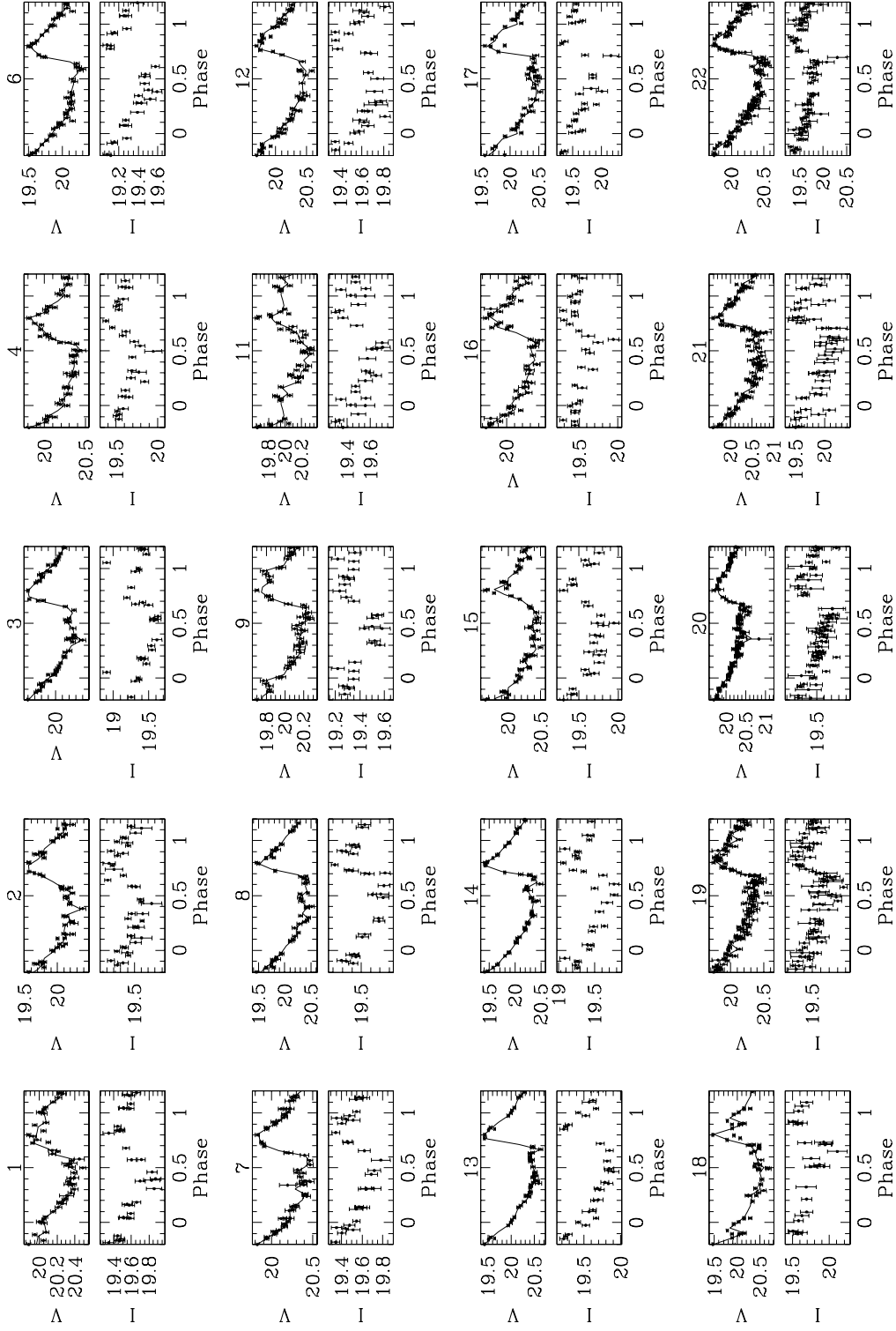


Fig. 4.— Phased light curves of the Draco RRL population. We present a sample of these light curves here. The full figure is provided in the online version of this paper.

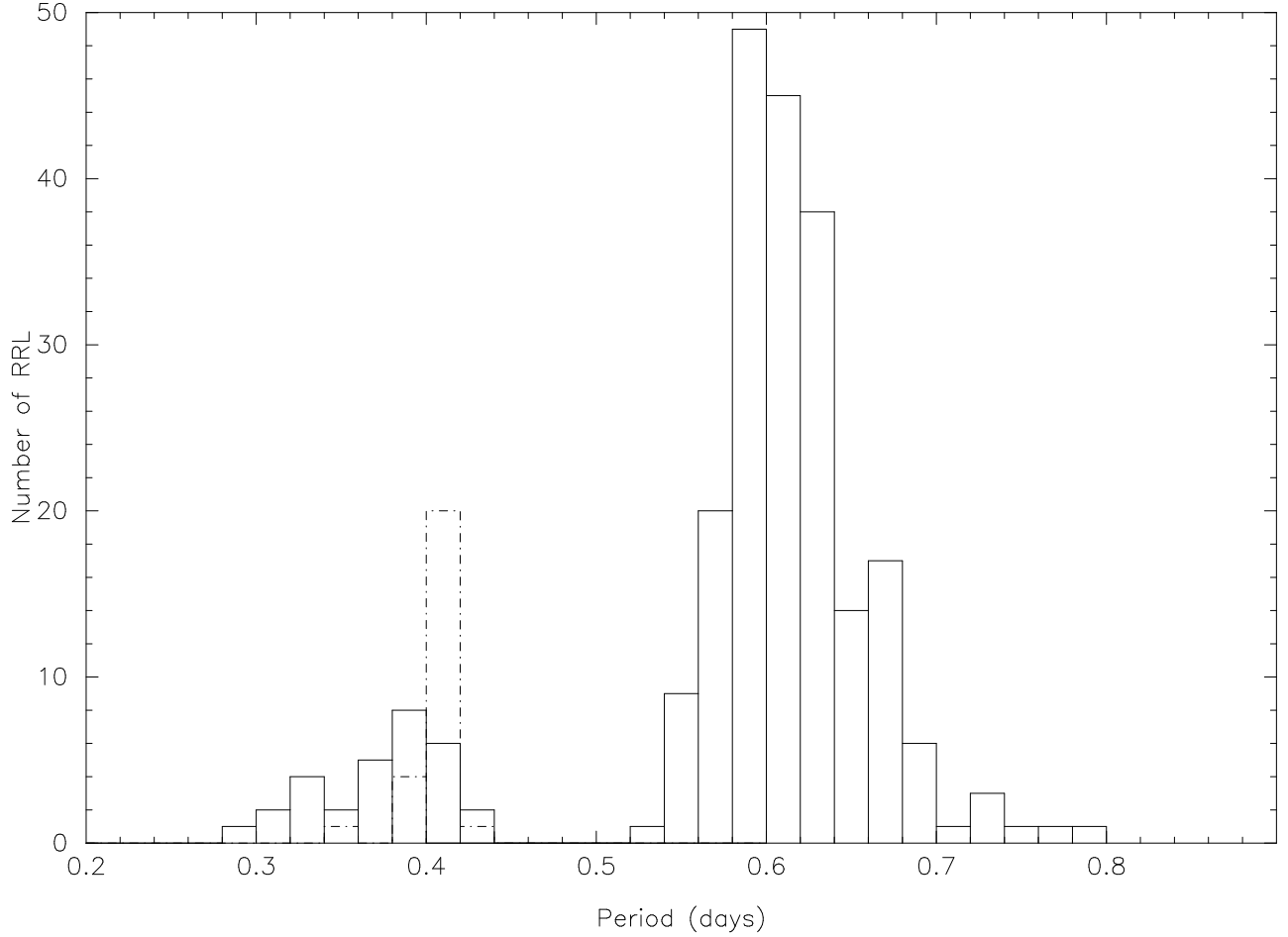
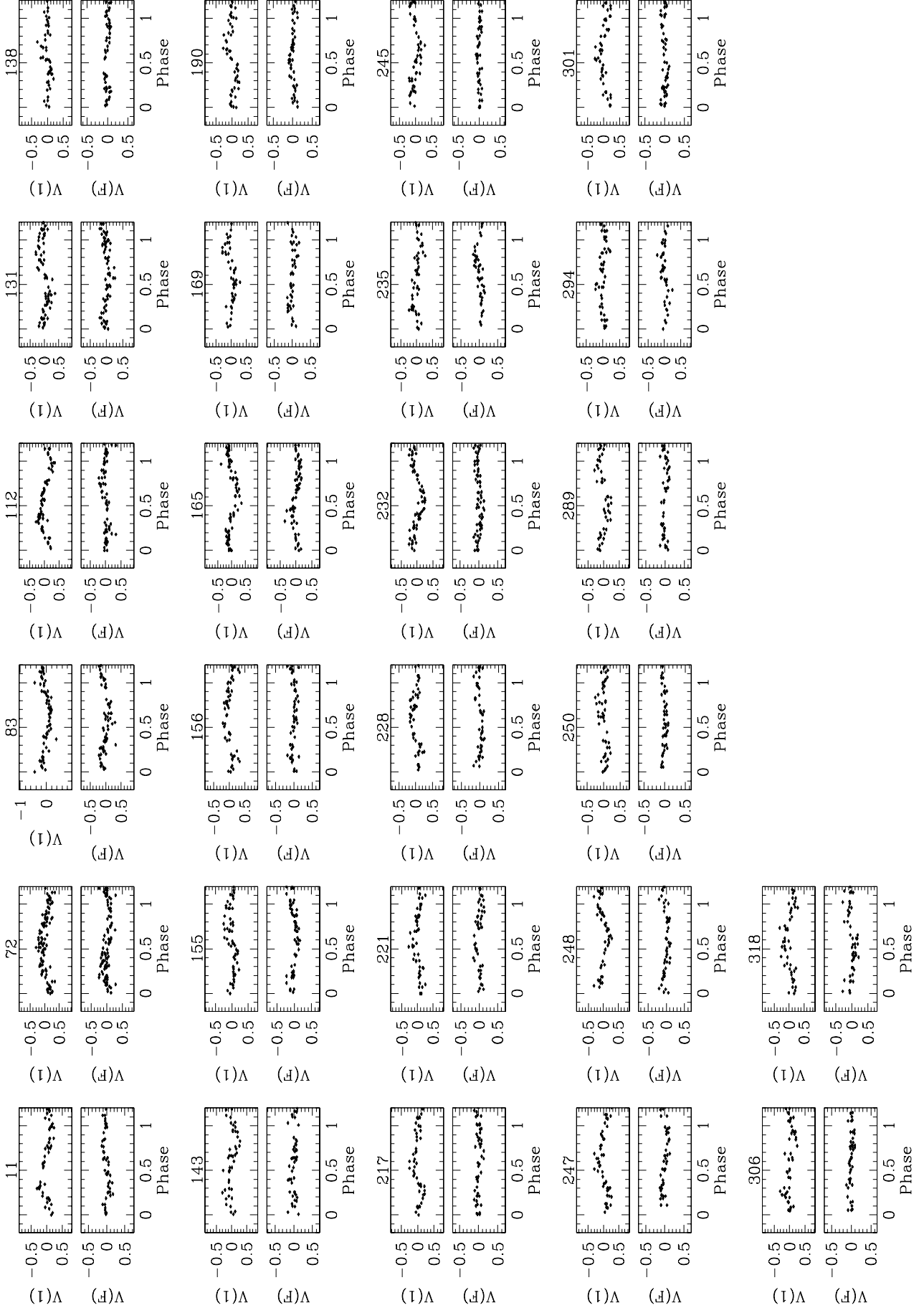


Fig. 5.— Period distribution of all Draco RR Lyrae stars. The dash-dot histogram is of the double-mode RR Lyraes. Average periods for each Bailey type of RRL: $\langle P_{ab} \rangle = 0.615d$, $\langle P_c \rangle = 0.375d$, $\langle P_d \rangle = 0.407d$.



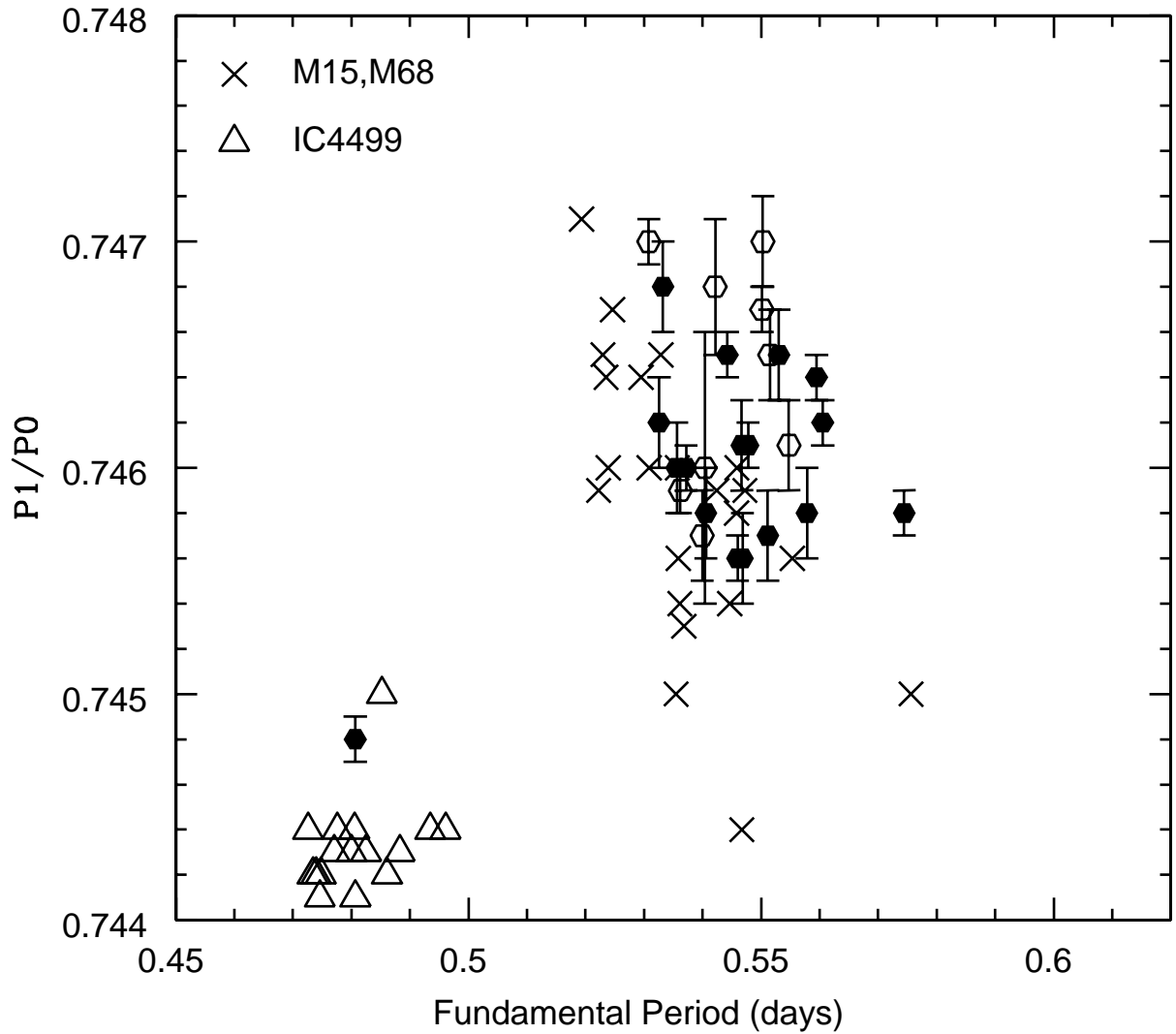


Fig. 7.— Petersen diagram of Draco RRd stars. The Draco RRd stars with uncertainties in the period are plotted as open circles. For comparison, RRd stars from the Oosterhoff type II clusters M15 (Nemec (1985b); Purdue et al. (1995)) and M68 (Walker 1994) and Oosterhoff type I cluster IC 4499 (Walker & Nemec 1996) are included.

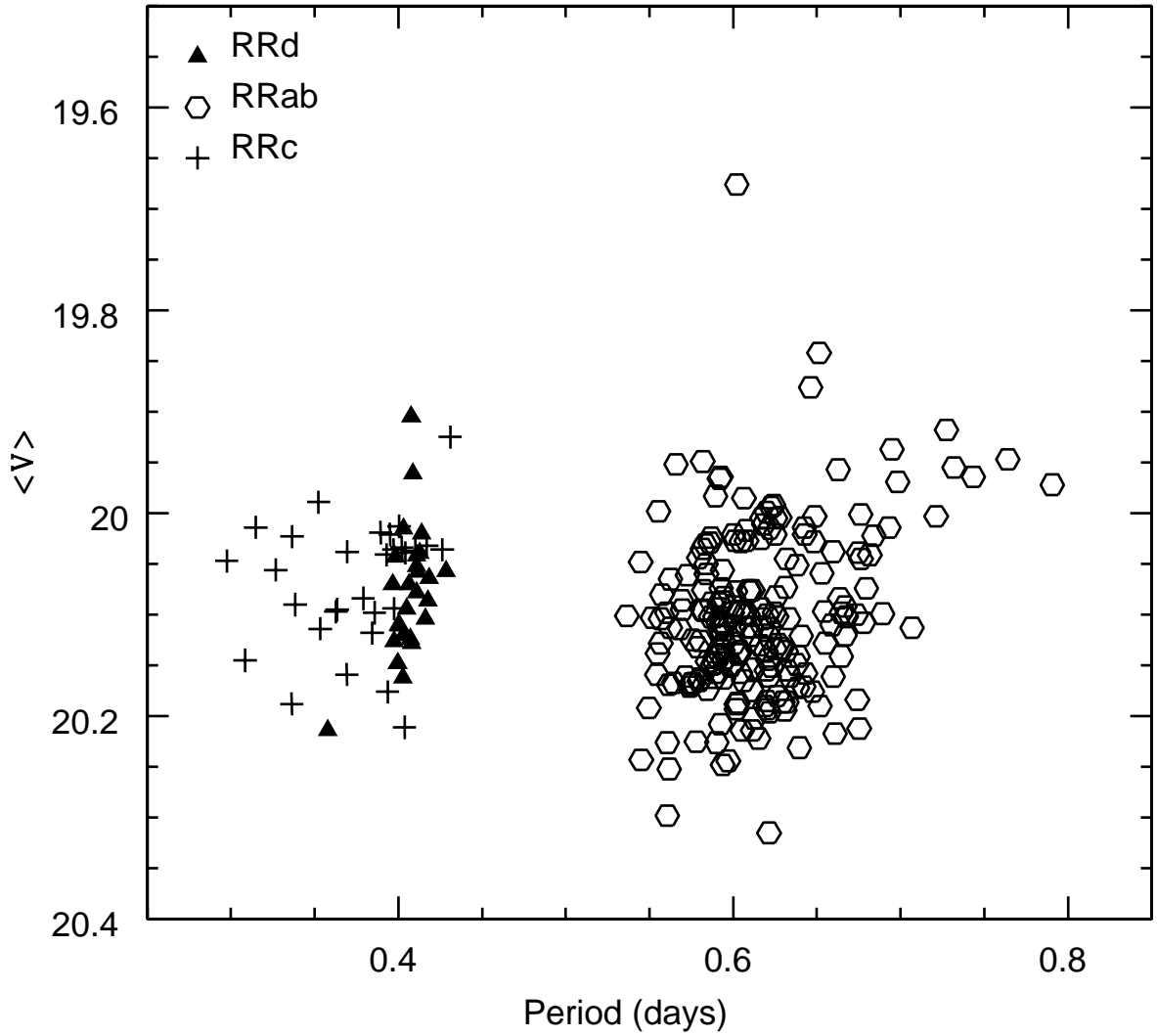


Fig. 8.— The intensity weighted mean V magnitude is plotted against period for all RRL stars in our study. Open circles are the RRab, plus signs are the RRc, and the filled triangles are the RRd stars.

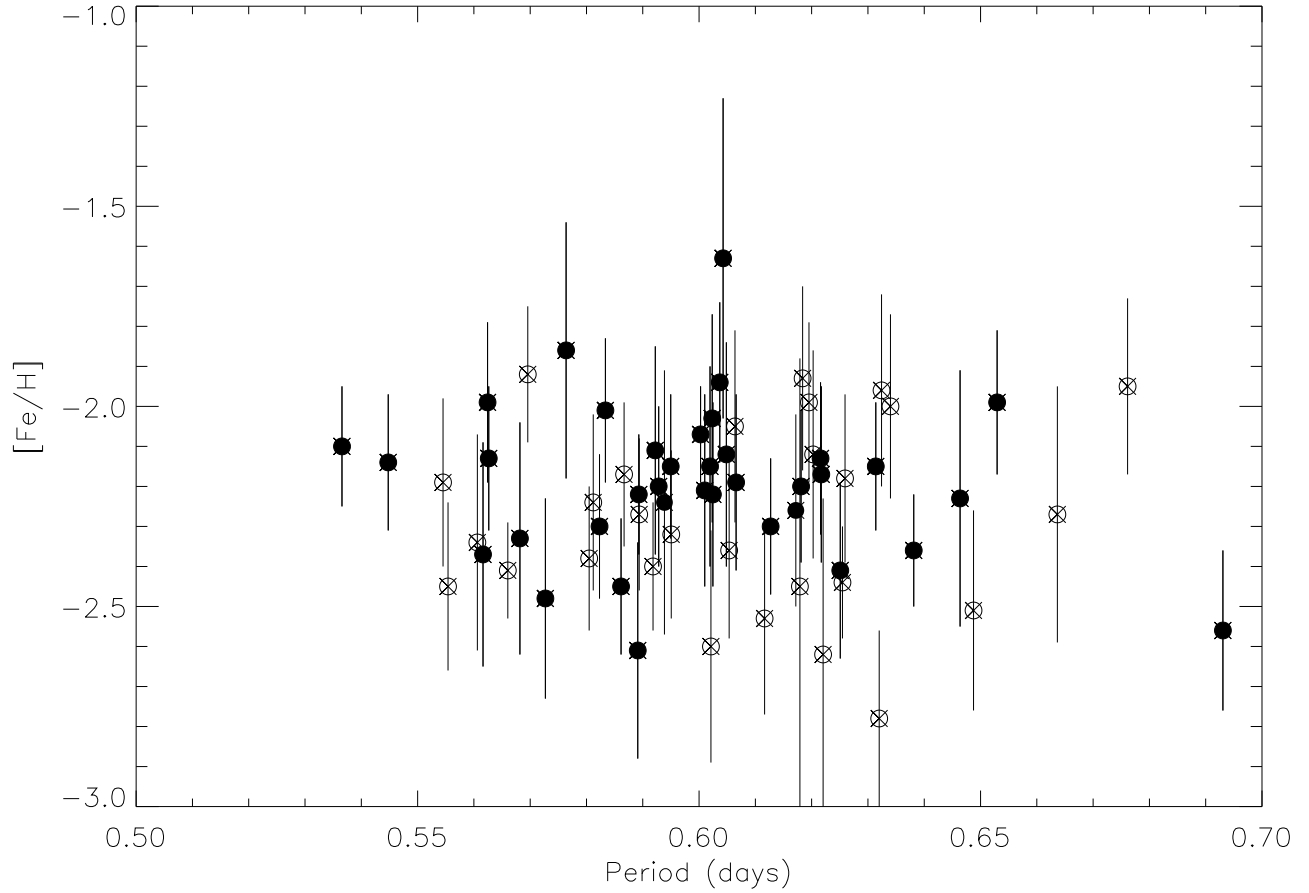


Fig. 9.— Metallicity distribution with respect to period for 63 Draco RRab stars. $[Fe/H]$ values were determined via the empirical method described in Jurcsik & Kovacs (1996). The filled points correspond to $D_M < 3.0$ and the open points are for $3.0 < D_M < 5.0$.

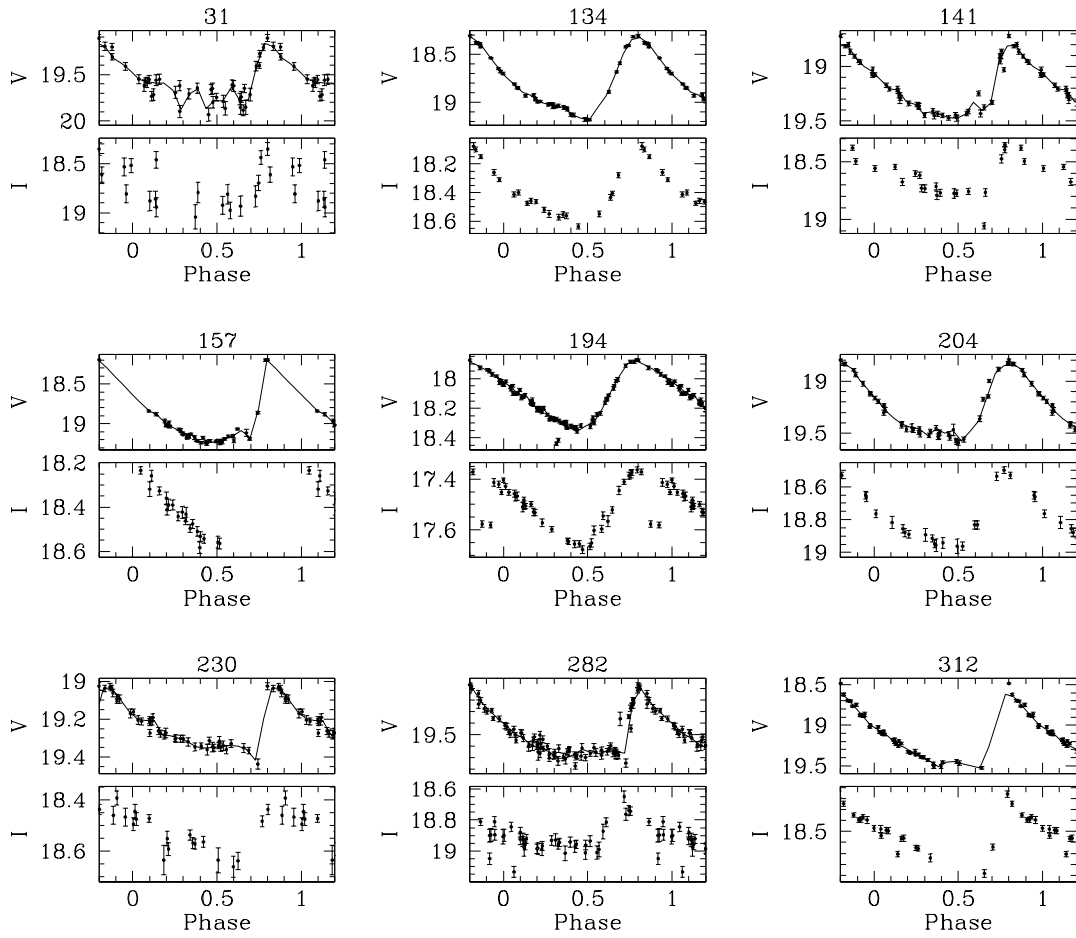


Fig. 10.— Phased light curves of the Draco anomalous Cepheids.

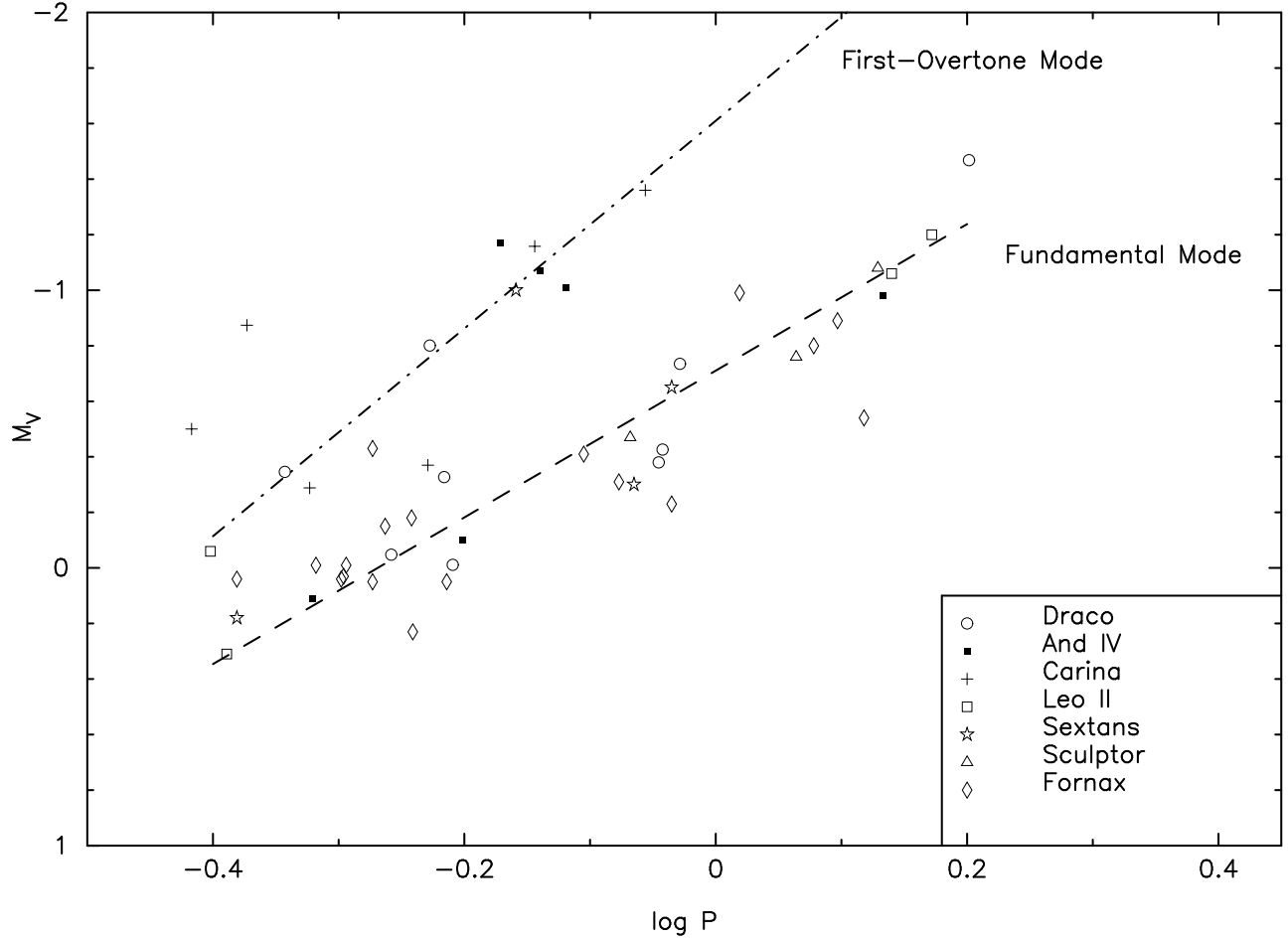


Fig. 11.— Draco anomalous Cepheids with respect to other anomalous Cepheids found in dSph galaxies. Information of anomalous Cepheids of other dwarf galaxies are from Pritzl et al. (2002a); Dall’Ora et al. (2003). Period-luminosity relations for the fundamental and first overtone pulsational modes from Pritzl et al. (2002a) are included.

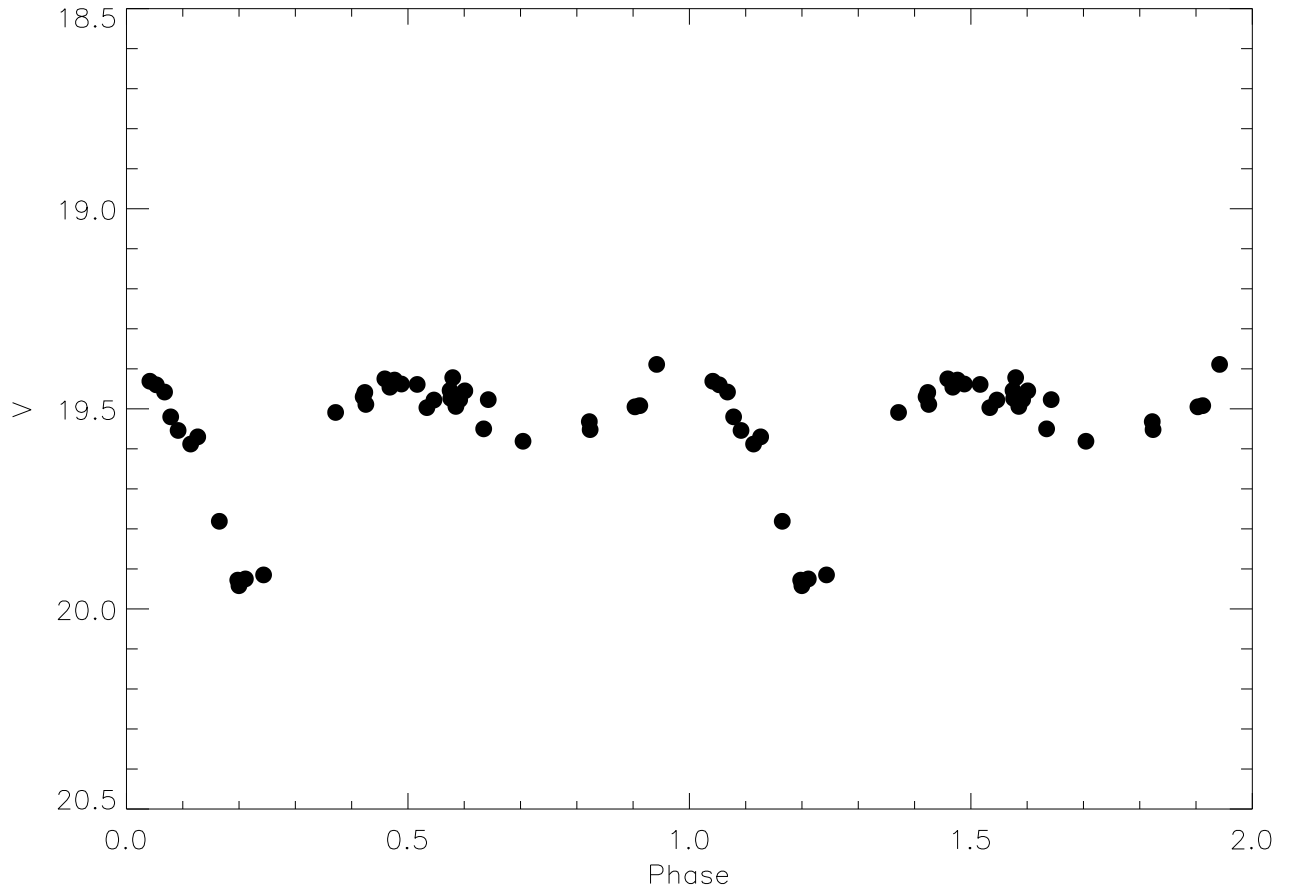


Fig. 12.— Field eclipsing binary star found in Bonanos et al. (2004) (their ID:J171906.2+574120.9) and in this work (our ID: V296). Period is 0.2435 days, which agrees well with their derived period.

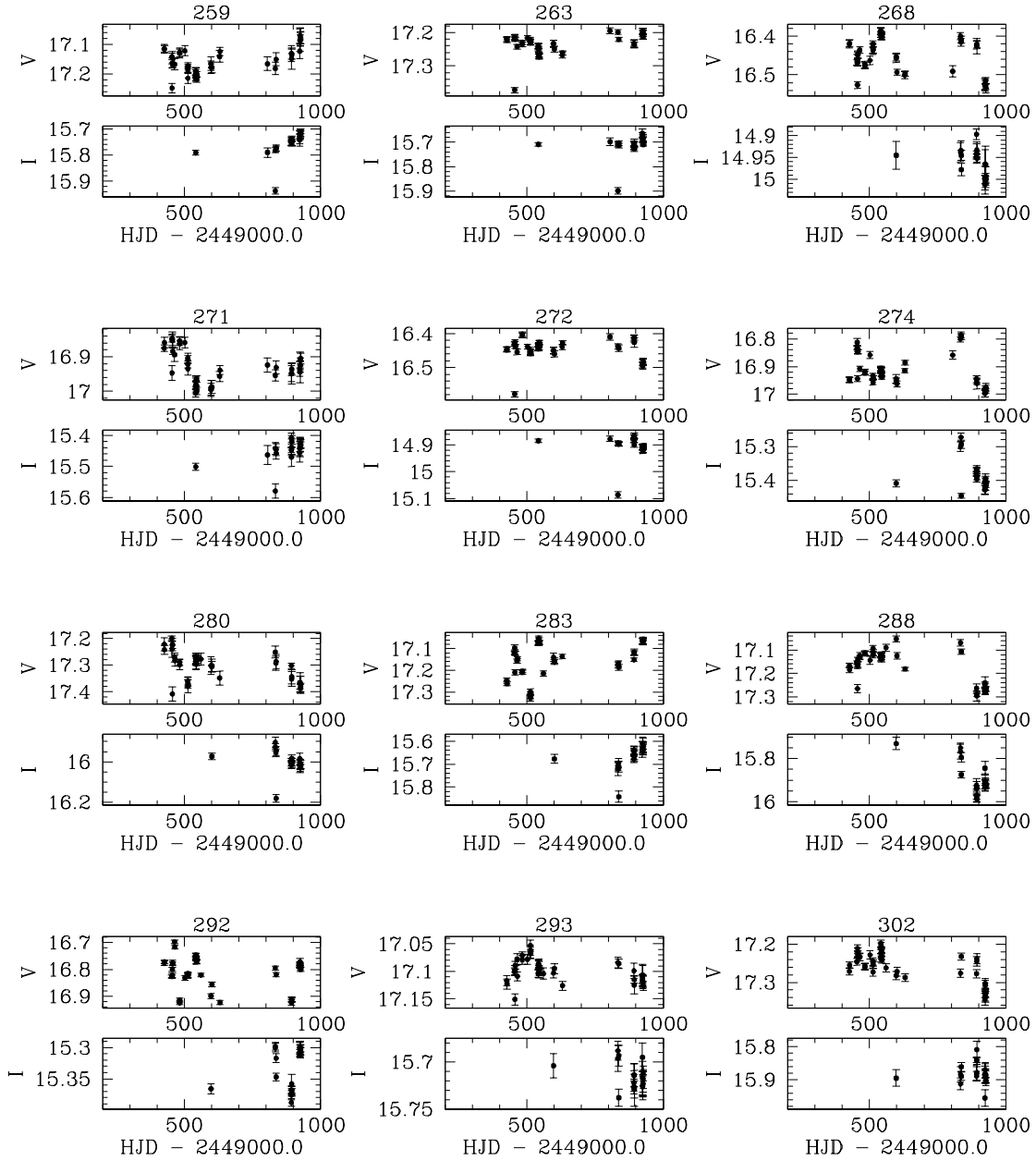


Fig. 13.— Time series data of the long period variable stars found in our survey. The x-axis is the heliocentric Julian date (HJD-2449000.0).

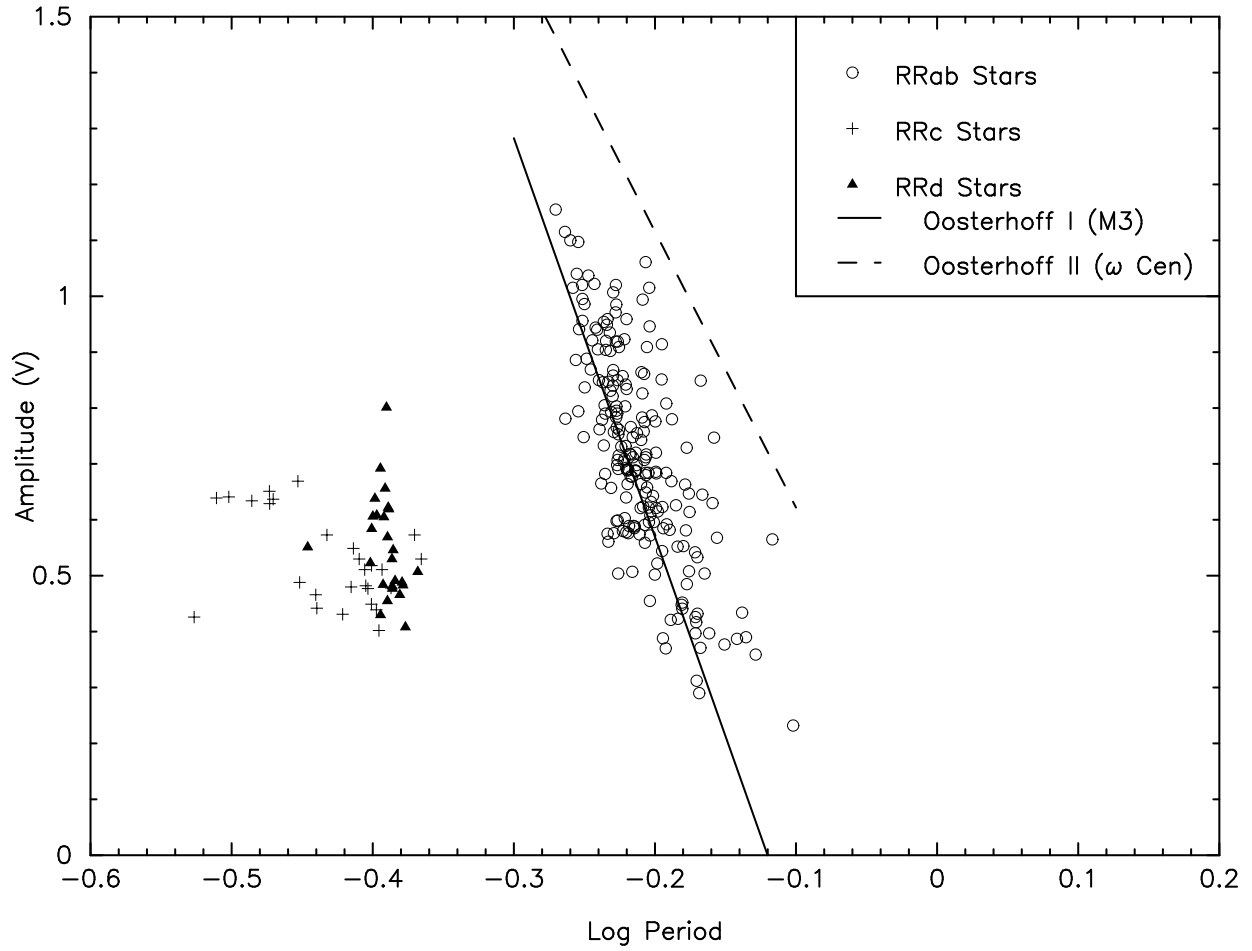


Fig. 14.— Period-amplitude diagram of the Draco RRL stars. Clement & Rowe (2000)’s relations for Oo I and Oo II are plotted to guide the eye for the Oosterhoff classification.

Table 1. Observations of Draco dwarf galaxy in Heliocentric Julian date (2449000.0 + days).

Year	USNO	WIRO
1993	–	183 - 187
1994	424 - 427	–
	453 - 456	–
	463 - 464	–
	482	–
	501	–
	512	511 - 513
	541 - 544	–
	560	–
1995	597 - 600	–
	629 - 630	–
	804 - 805	–
	833 - 836	–
	892 - 893	–
	923 - 926	–

Table 2. Stars in the Draco field not observed or found not to be variable.

B&S id	RA (2000.0)	DEC (2000.0)	Comments
V333	17:17:24.0	58:02:32.0	West of USNO fields
V5	17:20:20.4	58:00:55.0	In the gap between Quad 1 & 4 (P = 0.57006d)
V117	17:20:21.1	58:05:43.0	In the gap between Quad 1 & 4, not measured by B&S 19
V10	17:20:23.9	57:58:44.0	In the gap between Quad 1 & 4, near bright star, not measured by B&S 1961.
V205	17:23:19.6	57:57:55.0	East of USNO fields
Non-variable stars			
V168	17:19:27.24	58:00:35.0	Outside central field. Not measured by B&S 1961
V195	17:20:27.61	57:52:58.7	Near bright star. Not measured by B&S 1961
V111	17:20:28.60	57:52:58.9	Near bright star. Not measured by B&S 1961

Table 3. Transformation coefficients for USNO dataset

Filter	Obs. date	C_0	C_1	C_2	σ_{stds}
USNO V	08 Jul 1994	4.938	0.000	0.161	0.008
	24 Jun 1995	4.885	0.010	0.170	0.015
	25 Jun 1995	4.885	0.010	0.177	0.014
	23 Jun 1998	3.720	0.014	0.126	0.016
USNO I	08 Jul 1994	5.480	0.029	0.062	0.008
	24 Jun 1995	5.390	0.039	0.076	0.020
	25 Jun 1995	5.390	0.039	0.079	0.019
	23 Jun 1998	4.408	0.024	0.054	0.010

Table 4. Transformation coefficients for WIRO dataset^a

Field	α_V	α_I
WIRO Field 1	-3.453 ± 0.002	-1.734 ± 0.003
WIRO Field 2	-3.421 ± 0.002	-1.715 ± 0.002
WIRO Field 3	-3.426 ± 0.002	-1.769 ± 0.003

^aThe β coefficient is 0.081 ± 0.01 and $\gamma = -0.09 \pm 0.01$ in Equation 2.

Table 5. Properties of Draco RRL stars.

ID	RA (2000.0)	DEC (2000.0)	Period (days)	Amp	$\langle V \rangle^a$	$\langle I \rangle^a$	Type ^b
1	17:20:13.59	58:05:24.2	0.39363	0.48	20.18	19.60	c,BI?
2	17:19:42.54	58:03:26.8	0.59259	0.80	19.96	19.41	ab
3	17:20:14.88	58:01:46.8	0.64876	0.78	20.00	19.39	ab;B04
4	17:20:29.95	58:00:57.7	0.62625	0.61	20.18	19.63	ab;B04
6	17:20:18.95	58:00:37.9	0.69485	0.75	19.94	19.34	ab;B04
7	17:20:09.56	57:59:57.4	0.61896	0.62	20.19	19.57	ab;B04
8	17:20:15.23	57:59:17.3	0.56957	0.92	20.10	19.55	ab;B04
9	17:19:35.72	57:58:32.2	0.68418	0.50	20.02	19.39	ab;B04
11	17:20:41.93	57:58:27.4	0.41100	0.48	20.08	19.52	d;B04
12	17:20:41.86	57:57:50.0	0.57638	0.76	20.17	19.61	ab;B04
13	17:20:47.19	57:57:59.5	0.53657	1.16	20.10	19.64	ab;B04
14	17:19:30.51	57:56:33.8	0.61839	0.99	20.01	19.45	ab;B04
15	17:19:23.29	57:55:55.9	0.57803	0.67	20.23	19.63	ab,BI?;B04
16	17:19:56.68	57:56:00.6	0.62489	0.60	20.13	19.52	ab
17	17:20:40.33	57:56:04.1	0.59852	0.86	20.15	19.66	ab;B04
18	17:19:34.07	57:55:35.7	0.54963	1.10	20.19	19.73	ab,BI;B04
19	17:19:43.94	57:55:09.6	0.63183	0.69	20.14	19.53	ab;B04
20	17:19:48.26	57:54:51.4	0.61997	0.86	20.16	19.49	ab;B04
21	17:20:32.52	57:55:09.6	0.56061	0.99	20.30	19.88	ab;B04
22	17:19:11.96	57:54:37.2	0.58047	0.73	20.16	19.65	ab,BI?;B04
23	17:19:22.90	57:54:11.8	0.61791	0.78	20.11	19.55	ab,BI?;B04
24	17:19:58.92	57:54:14.7	0.63211	0.62	20.19	19.62	ab
25	17:20:49.78	57:54:05.1	0.56174	0.86	20.25	19.74	ab;B04
26	17:21:16.56	57:53:31.9	0.60392	0.69	20.14	19.47	ab,BI?;B04
27	17:20:06.01	57:53:49.0	0.76413	0.56	19.95	19.32	ab;B04
28	17:19:24.53	57:53:36.4	0.62593	0.57	20.10	19.47	ab;B04
29	17:20:16.66	57:53:12.1	0.56919	0.89	20.09	19.33	ab;B04
30	17:20:53.28	57:53:14.2	0.62977	0.60	20.19	19.58	ab;B04
32	17:19:56.27	57:52:47.8	0.55184	1.01	20.10	19.55	ab,BI?

Table 5—Continued

ID	RA (2000.0)	DEC (2000.0)	Period (days)	Amp	$\langle V \rangle^a$	$\langle I \rangle^a$	Type ^b
33	17:19:52.43	57:52:26.5	0.61087	0.69	20.11	19.49	ab
34	17:20:16.96	57:52:40.2	0.54511	0.78	20.24	19.70	ab;B04
35	17:20:38.39	57:52:35.9	0.57488	0.91	20.17	19.59	ab,BI?;B04
36	17:20:17.63	57:52:00.7	0.62547	0.95	20.01	19.42	ab;B04
37	17:20:08.44	57:52:03.3	0.55452	0.89	20.16	19.64	ab;B04
38	17:19:47.67	57:51:41.6	0.62148	0.71	20.16	19.57	ab,BI?
39	17:19:55.37	57:51:37.6	0.57422	0.94	20.17	19.62	ab,BI?
40	17:20:36.85	57:52:12.9	0.61640	0.62	20.13	19.56	ab;B04
41	17:20:42.87	57:51:28.9	0.57880	0.78	20.13	19.55	ab,BI?;B04
42	17:19:21.80	57:51:21.4	0.69306	0.63	20.01	19.34	ab
43	17:20:05.77	57:51:07.8	0.60368	0.69	20.10	19.54	ab
44	17:20:16.89	57:50:18.2	0.38436	0.48	20.12	19.63	c
45	17:19:34.99	57:50:47.8	0.58048	0.95	20.13	19.55	ab
46	17:19:36.43	57:49:30.0	0.33633	0.65	20.19	19.73	c;B04
47	17:19:28.93	57:49:17.2	0.63242	0.68	20.16	19.52	ab;B04
48	17:19:49.91	57:49:04.6	0.58167	0.68	20.04	19.55	ab,BI?;B04
49	17:20:08.55	57:47:28.5	0.62026	0.71	20.10	19.52	ab;B04
50	17:19:38.37	57:47:24.7	0.37904	0.43	20.08	19.65	c;B04
51	17:21:15.59	58:05:21.9	0.60658	0.77	20.10	19.53	ab
52	17:20:59.26	58:05:22.9	0.60143	0.73	20.08	19.47	ab
53	17:20:41.85	58:03:45.2	0.64255	0.68	20.01	19.42	ab,BI?
54	17:19:03.26	58:03:07.7	0.63874	0.62	20.14	19.57	ab
55	17:19:59.50	58:03:34.4	0.60100	0.80	20.03	19.50	ab
56	17:21:14.16	58:03:17.2	0.59356	0.85	20.06	19.53	ab
57	17:20:08.17	58:02:31.7	0.60485	0.59	20.03	19.38	ab
58	17:20:06.14	58:02:06.6	0.60427	0.58	20.16	19.54	ab;B04
59	17:20:02.26	58:01:20.6	0.58929	0.86	20.15	19.59	ab
60	17:19:24.78	57:58:47.4	0.60930	0.59	20.08	19.45	ab;B04
61	17:21:30.12	57:58:41.1	0.38941	0.53	20.02	19.50	c
62	17:20:57.20	57:58:21.3	0.60347	0.66	20.14	19.55	ab;B04

Table 5—Continued

ID	RA (2000.0)	DEC (2000.0)	Period (days)	Amp	$\langle V \rangle^a$	$\langle I \rangle^a$	Type ^b
63	17:20:46.55	57:57:41.8	0.61063	0.59	20.12	19.52	ab;B04
64	17:19:31.78	57:57:05.1	0.59874	0.58	20.15	19.52	ab,Bl?;B04
65	17:19:59.22	57:56:46.5	0.58911	0.84	20.10	19.59	ab
66	17:19:05.65	57:55:20.2	0.64745	0.42	20.18	19.57	ab;B04
67	17:21:31.31	57:55:04.7	0.58752	0.79	20.15	19.62	ab,Bl
68	17:20:09.24	57:54:38.5	0.61683	0.66	20.03	19.43	ab,Bl?;B04
69	17:21:26.95	57:54:19.6	0.59496	0.76	20.11	19.52	ab
70	17:21:07.10	57:54:08.9	0.62508	1.01	20.02	19.45	ab;B04
71	17:20:15.59	57:54:18.0	0.62146	1.06	20.32	19.67	ab,Bl;B04
72	17:20:12.44	57:54:11.4	0.40715	0.99	20.12	19.64	d;B04
73	17:19:17.57	57:53:32.7	0.58470	0.85	20.17	19.61	ab;B04
74	17:20:00.32	57:53:26.4	0.59173	0.97	20.09	19.57	ab
75	17:20:56.66	57:53:52.5	0.60288	0.69	20.19	19.61	ab,Bl?;B04
76	17:18:58.17	57:52:56.7	0.58336	0.95	20.03	19.52	ab;B04
77	17:19:45.55	57:52:41.0	0.63960	0.58	20.23	19.65	ab,Bl?;B04
78	17:19:54.55	57:52:56.1	0.59315	0.70	20.12	19.56	ab,Bl?
79	17:19:54.93	57:52:28.0	0.61144	0.69	20.18	19.56	ab,Bl?
80	17:21:02.69	57:52:50.6	0.60234	0.96	20.14	19.71	ab;B04
81	17:20:21.07	57:52:19.0	0.73202	0.39	19.95	19.37	ab;B04
82	17:20:41.68	57:49:52.0	0.59222	0.78	20.14	19.57	ab
83	17:20:48.80	57:50:01.8	0.40078	0.61	20.11	19.54	d
84	17:19:53.42	57:48:45.6	0.59195	1.02	19.97	19.49	ab;B04
85	17:19:51.29	57:48:43.7	0.61164	0.72	20.08	19.50	ab;B04
86	17:19:46.23	57:47:44.4	0.62896	0.64	20.13	19.57	ab,Bl?;B04
87	17:21:08.69	57:47:46.6	0.61526	0.57	20.22	19.62	ab;B04
88	17:20:10.69	57:45:59.0	0.60195	0.64	20.19	19.65	ab;B04
89	17:20:09.22	57:45:38.1	0.60867	0.71	20.10	19.54	ab,Bl?;B04
90	17:19:45.89	58:05:18.7	0.30851	0.64	20.14	19.80	c
92	17:19:39.52	58:02:46.8	0.56437	0.89	20.17	19.62	ab,Bl?
93	17:19:49.13	58:02:12.5	0.58668	0.90	20.10	19.58	ab

Table 5—Continued

ID	RA (2000.0)	DEC (2000.0)	Period (days)	Amp	$\langle V \rangle^a$	$\langle I \rangle^a$	Type ^b
94	17:20:52.12	58:01:25.7	0.56032	1.02	20.10	19.54	ab;B04
95	17:21:07.01	57:59:42.4	0.61719	0.86	20.01	19.43	ab,BI?;B04
96	17:21:03.54	57:59:50.7	0.58401	0.57	20.06	19.45	ab,BI?;B04
97	17:20:59.14	58:00:05.8	0.31477	0.64	20.01	19.61	c;B04
98	17:20:07.12	57:59:49.4	0.62786	0.79	20.00	19.46	ab;B04
100	17:19:29.46	57:58:25.7	0.74363	0.36	19.96	19.36	ab;B04
101	17:19:39.07	57:58:04.0	0.61953	0.76	20.14	19.57	ab;B04
102	17:19:19.50	57:57:38.9	0.58258	0.92	20.08	19.54	ab;B04
103	17:20:28.25	57:57:00.8	0.60638	0.68	20.17	19.66	ab;B04
104	17:19:45.84	57:56:26.1	0.59182	0.92	20.11	19.55	ab;B04
105	17:21:31.28	57:55:10.1	0.61174	0.69	20.21	19.61	ab,BI?
106	17:20:26.69	57:54:27.5	0.62048	0.59	20.19	19.65	ab,BI;B04
107	17:19:26.62	57:53:34.2	0.58120	0.81	20.10	19.55	ab;B04
108	17:19:56.89	57:53:50.1	0.65976	0.44	20.16	19.52	ab,BI?
109	17:18:58.72	57:52:57.1	0.59473	0.71	20.13	19.52	ab;B04
110	17:19:18.40	57:52:45.6	0.36924	0.53	20.16	19.63	c;B04
112	17:21:06.42	57:51:52.9	0.42845	0.51	20.06	19.48	d;B04
113	17:20:03.11	57:49:51.9	0.36274	0.47	20.10	19.62	c
114	17:19:55.40	57:49:00.7	0.64636	0.58	19.88	19.29	ab;B04
115	17:19:02.18	57:47:54.5	0.59372	0.71	20.14	19.62	ab,BI?;B04
116	17:19:27.08	57:46:54.1	0.57984	0.90	20.16	19.64	ab;B04
118	17:20:59.32	58:01:26.4	0.58940	0.87	19.98	19.43	ab,BI;B04
119	17:20:25.90	58:00:02.2	0.66464	0.48	20.10	19.53	ab;B04
120	17:18:58.80	57:58:05.6	0.40051	0.44	20.01	19.51	c;B04
121	17:19:39.88	57:57:53.6	0.33647	0.63	20.02	19.55	c;B04
122	17:19:57.18	57:58:19.8	0.63837	0.54	20.17	19.59	ab
123	17:20:11.53	57:58:02.6	0.58474	0.56	20.15	19.61	ab,BI;B04
124	17:20:33.07	57:57:30.7	0.55673	1.10	20.13	19.62	ab;B04
125	17:20:53.49	57:57:04.6	0.68171	0.65	20.04	19.44	ab;B04
126	17:20:08.90	57:56:22.9	0.59283	0.77	20.07	19.49	ab;B04

Table 5—Continued

ID	RA (2000.0)	DEC (2000.0)	Period (days)	Amp	$\langle V \rangle^a$	$\langle I \rangle^a$	Type ^b
127	17:19:44.97	57:54:18.1	0.66454	0.73	20.14	19.57	ab;B04
128	17:21:14.05	57:54:35.5	0.63400	0.61	20.16	19.54	ab;B04
129	17:19:41.43	57:53:27.6	0.59012	0.58	20.23	19.66	ab;B04
130	17:21:19.05	57:53:24.5	0.57159	1.02	20.16	19.57	ab,BI;B04
131	17:21:19.47	57:52:35.7	0.40621	0.66	20.07	19.57	d;B04
132	17:20:24.20	57:51:41.3	0.63331	0.52	20.10	19.55	ab;B04
133	17:20:51.20	57:51:47.8	0.61001	0.58	20.08	19.49	ab;B04
135	17:20:30.16	57:50:40.1	0.63139	0.78	20.07	19.46	ab
136	17:20:44.12	57:50:27.0	0.55487	1.19	20.14	19.56	ab
137	17:19:23.01	57:49:58.5	0.60245	0.83	20.19	19.59	ab;B04
138	17:20:35.88	57:49:18.7	0.40773	0.46	19.91	19.30	d
139	17:21:21.90	57:49:26.8	0.33841	0.64	20.09	19.70	c
140	17:20:17.09	57:46:41.0	0.62578	0.51	20.08	19.53	ab;B04
142	17:19:13.30	58:04:54.5	0.63813	0.91	20.05	19.51	ab
143	17:19:31.77	57:59:27.1	0.40324	0.43	20.02	19.14	d;B04
144	17:19:52.18	57:59:09.4	0.58887	0.82	20.16	19.59	ab,BI?;B04
145	17:20:57.87	57:58:48.5	0.39738	0.52	20.09	19.61	c;B04
146	17:21:26.73	57:57:25.9	0.58186	0.79	19.95	19.38	ab,BI
147	17:19:48.75	57:56:57.0	0.58732	0.66	20.09	19.47	ab,BI;B04
148	17:19:56.80	57:54:59.0	0.67413	0.40	20.18	19.60	ab,BI?
149	17:19:22.46	57:54:04.3	0.67536	0.31	20.21	19.61	ab;B04
150	17:20:31.38	57:53:02.4	0.67633	0.43	20.05	19.31	ab;B04
151	17:20:53.13	57:53:03.7	0.62067	0.56	20.14	19.51	ab;B04
152	17:20:02.61	57:51:30.6	0.62690	0.63	20.13	19.56	ab,BI?
153	17:20:17.46	57:46:01.8	0.40215	0.40	20.03	19.51	c;B04
154	17:20:50.94	57:45:17.0	0.63200	0.72	20.05	19.46	ab;B04
155	17:20:03.72	58:05:21.6	0.41989	0.41	20.02	19.54	d
156	17:19:55.09	58:01:09.9	0.40871	0.62	19.96	19.54	d
158	17:20:31.15	57:57:37.2	0.65465	0.55	20.10	19.53	ab,BI;B04
159	17:19:05.65	57:55:38.8	0.65295	0.63	20.06	19.46	ab;B04

Table 5—Continued

ID	RA (2000.0)	DEC (2000.0)	Period (days)	Amp	$\langle V \rangle^a$	$\langle I \rangle^a$	Type ^b
160	17:20:08.92	57:55:29.3	0.64320	0.59	20.16	19.59	ab,BI;B04
161	17:20:40.59	57:54:52.1	0.62158	0.65	20.20	19.63	ab;B04
162	17:20:37.99	57:55:31.1	0.62171	0.68	20.11	19.37	ab;B04
163	17:20:58.94	57:53:44.2	0.56060	0.96	20.23	19.71	ab,BI;B04
164	17:20:45.14	57:51:27.7	0.62464	0.62	20.10	19.50	ab,BI?;B04
165	17:20:08.64	57:50:07.1	0.35802	0.55	20.21	19.64	d
166	17:21:20.23	57:49:18.2	0.36339	0.44	20.10	19.62	c
167	17:20:07.68	58:01:40.2	0.66756	0.61	20.10	19.51	ab;B04
169	17:20:42.33	57:58:52.4	0.40317	0.69	20.12	19.60	d;B04
170	17:20:52.01	57:55:32.0	0.40370	0.42	20.21	19.84	c;B04
171	17:20:15.40	57:53:28.1	0.59963	0.70	20.10	19.57	ab,BI?;B04
172	17:20:36.84	57:48:20.6	0.66282	0.66	19.96	19.37	ab;B04
173	17:20:59.52	57:55:42.3	0.36946	0.57	20.04	19.31	c;B04
174	17:19:42.91	57:55:27.1	0.67612	0.53	20.00	19.45	ab;B04
175	17:20:58.47	57:53:32.0	0.56243	0.99	20.11	19.61	ab;B04
176	17:20:48.99	57:51:03.2	0.60211	0.58	19.68	18.96	ab, blended?
177	17:20:52.79	57:50:41.8	0.59242	0.98	20.11	19.49	ab
178	17:20:57.24	57:50:01.2	0.59386	0.92	20.09	19.49	ab
179	17:21:10.77	57:47:36.2	0.39293	0.51	20.04	19.57	c;B04
180	17:20:46.73	58:03:03.2	0.65982	0.45	20.04	19.38	ab
181	17:21:12.74	58:01:31.0	0.38572	0.55	20.10	19.66	c;B04
182	17:19:28.21	58:00:43.5	0.41022	0.48	20.04	19.57	c;B04
183	17:21:07.35	57:58:00.6	0.59506	0.91	20.11	19.57	ab;B04
184	17:20:13.73	57:57:24.9	0.59430	0.69	20.08	19.54	ab,BI?
185	17:20:47.28	57:55:23.0	0.59385	0.60	20.25	19.62	ab,BI?;B04
186	17:20:06.57	57:49:45.0	0.59717	0.73	20.24	19.66	ab,BI?
187	17:19:26.12	57:48:51.3	0.68939	0.40	20.10	19.49	ab;B04
188	17:19:42.62	57:53:30.0	0.67368	0.54	20.10	19.47	ab;B04
189	17:21:13.02	57:53:50.8	0.59440	0.75	20.14	19.53	ab,BI?;B04
190	17:20:42.51	57:51:53.1	0.39652	0.52	20.07	19.54	d;B04

Table 5—Continued

ID	RA (2000.0)	DEC (2000.0)	Period (days)	Amp	$\langle V \rangle^a$	$\langle I \rangle^a$	Type ^b
191	17:19:17.45	57:48:42.9	0.39729	0.45	20.04	19.57	c;B04
192	17:20:13.14	57:55:26.4	0.66098	0.55	20.22	19.63	ab,Bl;B04
193	17:20:21.58	57:54:31.0	0.67818	0.29	20.11	19.53	ab,Bl;B04
196	17:19:51.33	57:53:20.9	0.58936	1.01	20.16	19.65	ab;B04
197	17:21:25.64	57:50:30.4	0.59265	0.60	20.12	19.51	ab,Bl
198	17:20:51.82	57:56:35.9	0.67956	0.37	20.07	19.46	ab;B04
199	17:21:18.63	57:47:43.8	0.66690	0.65	20.09	19.52	ab
200	17:21:17.02	58:05:11.9	0.41700	0.32	20.03	19.52	c
201	17:20:36.57	58:03:57.7	0.65900	0.45	20.11	19.50	ab
202	17:21:21.04	57:50:44.8	0.64213	0.37	20.17	19.50	ab,Bl?
207	17:23:05.77	57:59:13.4	0.56817	0.87	20.11	19.56	ab
213	17:22:41.11	57:58:03.8	0.62290	0.66	20.15	19.54	ab
216	17:22:30.47	57:42:24.1	0.59338	0.79	20.11	19.55	ab
217	17:22:22.09	57:58:02.7	0.41166	0.55	20.06	19.50	d
218	17:22:20.80	57:55:54.4	0.60842	0.75	20.11	19.53	ab
219	17:22:19.42	57:53:10.9	0.60534	0.63	20.21	19.62	ab
220	17:22:19.44	57:51:43.8	0.62203	0.72	20.12	19.52	ab
221	17:22:16.13	57:50:03.7	0.40788	0.57	20.13	19.54	d
223	17:22:09.97	57:46:40.5	0.60209	0.69	20.19	19.60	ab
225	17:22:03.62	57:43:59.2	0.57588	0.85	20.13	19.65	ab,Bl?
226	17:22:00.30	57:58:01.1	0.29750	0.43	20.05	19.66	c
227	17:22:00.12	57:58:23.4	0.60069	0.60	20.13	19.55	ab
228	17:21:48.28	58:11:29.1	0.41605	0.47	20.10	19.55	d
232	17:21:47.30	57:53:06.5	0.41082	0.53	20.05	19.47	d
233	17:21:46.39	58:07:32.8	0.59427	0.50	20.16	19.64	ab,Bl
234	17:21:45.75	57:51:49.5	0.65512	0.42	20.13	19.49	ab,Bl?
235	17:21:45.39	57:41:45.7	0.39954	0.64	20.15	19.71	d
236	17:21:42.85	57:37:02.0	0.40420	0.51	20.04	19.56	c
237	17:21:41.89	57:54:29.7	0.61271	0.76	20.20	19.67	ab
238	17:21:41.81	57:38:11.9	0.56264	0.84	20.07	19.51	ab

Table 5—Continued

ID	RA (2000.0)	DEC (2000.0)	Period (days)	Amp	$\langle V \rangle^a$	$\langle I \rangle^a$	Type ^b
239	17:21:41.23	57:55:43.5	0.59004	0.93	20.14	19.59	ab,Bl?
242	17:21:40.90	57:59:39.4	0.35332	0.49	20.11	19.70	c
243	17:21:41.15	57:54:23.9	0.72130	0.39	20.00	19.37	ab
244	17:21:40.66	57:54:36.2	0.56161	0.67	20.17	19.66	ab
245	17:21:40.34	57:51:32.2	0.41106	0.48	20.04	19.45	d
246	17:21:38.70	57:52:42.0	0.63086	0.50	20.19	19.56	ab,Bl?
247	17:21:36.46	57:55:58.8	0.41762	0.49	20.09	19.55	d
248	17:21:35.07	57:53:04.9	0.41828	0.48	20.06	19.51	d
249	17:21:30.07	58:07:48.5	0.60027	0.92	20.09	19.60	ab
250	17:21:30.37	57:48:52.8	0.40488	0.48	20.09	19.59	d
252	17:21:29.08	58:03:16.1	0.58232	0.90	20.10	19.54	ab
253	17:21:26.82	58:06:58.0	0.59247	0.80	20.21	19.68	ab,Bl
258	17:21:09.54	58:09:14.7	0.58614	0.94	20.03	19.47	ab
260	17:21:00.07	58:06:20.3	0.55743	0.94	20.08	19.56	ab
261	17:20:58.51	58:09:18.0	0.55670	0.79	20.10	19.55	ab
262	17:20:55.08	57:43:35.2	0.61697	0.74	20.09	19.53	ab
265	17:20:51.99	58:15:02.1	0.58396	0.96	20.05	19.60	ab,Bl
267	17:20:46.52	57:48:18.9	0.67495	0.42	20.04	19.41	ab,Bl
269	17:20:43.61	58:08:30.9	0.54478	1.11	20.05	19.54	ab
270	17:20:42.46	57:39:55.8	0.56602	1.04	19.95	19.41	ab
273	17:20:38.99	57:57:32.4	0.79061	0.23	19.97	19.36	ab
275	17:20:29.33	57:58:07.6	0.65198	0.32	20.19	19.64	ab
276	17:20:19.11	58:16:21.8	0.63478	0.43	17.57	16.88	ab;field
277	17:20:14.32	57:44:02.0	0.64281	0.81	20.02	19.49	ab,Bl
278	17:20:08.35	57:35:01.8	0.61812	0.83	20.10	19.60	ab
279	17:20:00.79	57:44:11.7	0.60644	0.72	19.99	19.43	ab
281	17:20:00.66	57:42:20.3	0.69818	0.58	19.97	19.39	ab
284	17:19:57.88	57:41:57.3	0.60760	0.68	20.02	19.45	ab
285	17:19:44.74	57:57:37.3	0.65136	0.57	19.84	19.27	ab;B04
286	17:19:43.55	58:06:02.9	0.60153	0.84	20.11	19.55	ab,Bl

Table 5—Continued

ID	RA (2000.0)	DEC (2000.0)	Period (days)	Amp	$\langle V \rangle^a$	$\langle I \rangle^a$	Type ^b
289	17:19:29.26	57:41:59.5	0.39742	0.58	20.13	19.64	d
290	17:19:23.22	58:08:20.3	0.70680	0.38	20.11	19.47	ab
291	17:19:21.05	57:36:41.4	0.72744	0.43	19.92	19.34	ab,BI?
294	17:19:08.98	57:34:06.7	0.40548	0.60	20.11	19.69	d,BI?
295	17:19:07.75	57:44:32.7	0.42625	0.57	20.04	19.61	c
297	17:19:04.96	58:03:30.3	0.66699	0.51	20.12	19.48	ab,BI?
298	17:19:04.47	58:06:17.1	0.63785	0.85	20.15	19.68	ab,BI?
301	17:19:00.43	57:37:29.9	0.41287	0.49	20.04	19.61	d
303	17:18:51.86	57:47:28.1	0.62029	0.78	20.19	19.68	ab
304	17:18:49.62	57:53:56.1	0.66365	0.58	20.08	19.51	ab;B04
305	17:18:47.75	58:03:31.9	0.64080	0.31	20.12	19.46	ab
306	17:18:47.01	58:14:08.9	0.39823	0.61	20.04	19.54	d
307	17:18:45.25	57:52:22.6	0.39504	0.48	20.02	19.57	c;B04
308	17:18:38.43	57:52:38.5	0.60803	0.51	20.03	19.49	ab;B04
309	17:18:35.08	57:56:54.8	0.61993	0.63	20.00	19.24	ab;B04
310	17:18:33.34	57:51:59.9	0.64819	0.67	20.03	19.45	ab
313	17:18:29.82	58:11:52.7	0.57270	0.94	20.06	19.52	ab
314	17:18:27.57	57:52:13.3	0.43096	0.53	19.93	19.44	c
315	17:18:24.82	57:59:48.3	0.57953	0.85	20.04	19.53	ab
316	17:18:24.92	57:43:31.7	0.32679	0.63	20.06	19.74	c
317	17:18:19.34	57:58:42.7	0.58685	0.83	20.02	19.48	ab,BI
318	17:18:19.52	57:55:49.9	0.40829	0.62	20.16	19.61	d
319	17:18:19.52	57:46:21.1	0.62276	0.91	19.99	19.45	ab,BI
321	17:18:12.87	58:02:56.0	0.59716	0.61	17.93	17.37	ab;field
323	17:18:09.26	57:37:05.7	0.55540	1.04	20.00	19.53	ab
324	17:18:04.66	58:02:35.7	0.60035	0.71	20.02	19.47	ab
325	17:18:02.69	57:48:14.2	0.62424	0.68	19.99	19.43	ab
326	17:17:59.11	58:02:05.6	0.62179	0.68	20.02	19.45	ab
327	17:17:55.93	57:40:00.0	0.61859	0.94	17.55	17.05	ab;field
330	17:17:46.91	57:43:27.8	0.35233	0.67	19.99	19.54	c

Table 5—Continued

ID	RA (2000.0)	DEC (2000.0)	Period (days)	Amp	$\langle V \rangle^a$	$\langle I \rangle^a$	Type ^b
332	17:17:29.12	57:34:25.6	0.61233	0.70	20.15	19.61	ab

^aIntensity-weighted magnitudes

^bBl = Blazhko effect

References. — B04 = Bonanos et al. (2004)

Table 6. Properties of the Draco RRd stars.

ID	P_1	Error	P_0	Error	P_1/P_0	Error ^a
11	0.41100	.00002	0.55114	.00010	0.7457	.0002
72	0.40711	.00002	0.54599	.00006	0.7456	.0001
83	0.40075	.00002	0.53720	.00006	0.7460	.0001
112	0.42844	.00002	0.57446	.00005	0.7458	.0001
131	0.40626	.00002	0.54424	.00006	0.7465	.0001
138	0.40773	.00003	0.54601	.00012	0.7467	.0002
143	0.40317	.00004	0.54042	.00003	0.7460	.0006*
155	0.41393	.00003	0.55476	.00009	0.7461	.0002*
156	0.40868	.00002	0.54778	.00006	0.7461	.0001
165	0.35798	.00002	0.48064	.00004	0.7448	.0001
169	0.40316	.00003	0.54059	.00008	0.7458	.0002
190	0.39652	.00001	0.53080	.00006	0.7470	.0001*
217	0.41166	.00003	0.55149	.00014	0.7465	.0002*
221	0.40788	.00003	0.54671	.00008	0.7461	.0002
228	0.41606	.00003	0.55784	.00010	0.7458	.0002
232	0.41081	.00001	0.55017	.00007	0.7467	.0001*
235	0.39954	.00003	0.53560	.00011	0.7460	.0002
245	0.41105	.00001	0.55029	.00010	0.7470	.0002*
247	0.41760	.00002	0.55946	.00006	0.7464	.0001
248	0.41828	.00002	0.56055	.00005	0.7462	.0001
250	0.40491	.00002	0.54218	.00014	0.7468	.0003*
289	0.39743	.00002	0.53258	.00008	0.7462	.0002
294	0.39998	.00002	0.53622	.00007	0.7459	.0001*
301	0.41286	.00002	0.55306	.00007	0.7465	.0002
306	0.39824	.00002	0.53323	.00009	0.7468	.0002
318	0.40264	.00004	0.53995	.00007	0.7457	.0002*

^aStars with an * denote some uncertainty with the period solutions due to aliasing.

Table 7. Fourier decomposition parameters for RRab stars.

ID	A_0	R_{21}	R_{31}	R_{41}	ϕ_{21}	ϕ_{31}	ϕ_{41}	$\sigma_{\phi_{31}}$	[Fe/H]	$\sigma_{[Fe/H]}$	D_M pass? ^a
2	20.9797	0.3221	0.0858	0.1693	3.5756	1.403	5.449	0.553	-2.43	0.75	
3	21.0260	0.3453	0.2780	0.2168	3.9108	1.569	6.036	0.180	-2.51	0.25	*
4	21.1916	0.4781	0.1509	0.0581	3.8671	1.302	1.641	0.356	-2.76	0.48	
6	20.9611	0.5028	0.2893	0.1936	3.8149	2.042	6.092	0.134	-2.11	0.18	
7	21.2041	0.4867	0.3420	0.0415	3.7750	1.915	5.866	0.179	-1.86	0.24	
8	21.1371	0.5084	0.3504	0.2033	3.8696	1.671	6.105	0.128	-1.92	0.17	*
9	21.0360	0.4902	0.2396	0.1688	3.7757	1.799	0.785	0.222	-2.39	0.30	
12	21.2055	0.4099	0.2215	0.1029	3.8709	1.743	5.930	0.238	-1.86	0.32	*
13	21.1566	0.4181	0.2999	0.1742	3.8595	1.408	5.677	0.108	-2.10	0.15	*
14	21.0536	0.3410	0.3305	0.3288	3.8314	1.857	5.995	0.173	-1.93	0.23	*
15	21.2359	0.4504	0.2656	0.0374	3.5087	1.533	5.400	0.278	-2.16	0.38	*
16	21.1378	0.3367	0.1520	0.0652	4.0760	1.823	4.995	0.453	-2.02	0.61	
17	21.1852	0.3700	0.2613	0.0471	3.5913	1.052	6.038	0.272	-2.96	0.37	
19	21.1497	0.4018	0.2557	0.1974	4.1254	2.255	0.236	0.186	-1.45	0.25	
20	21.1713	0.4051	0.3398	0.2134	3.8324	1.714	0.185	0.159	-2.15	0.22	
21	21.3392	0.3626	0.2600	0.2263	3.7277	1.337	5.622	0.199	-2.34	0.27	*
22	21.1894	0.3796	0.3104	0.1628	4.1072	1.950	0.004	0.286	-1.59	0.39	
23	21.1370	0.5135	0.2314	0.2189	3.7667	1.487	5.489	0.425	-2.45	0.57	
24	21.1933	0.3830	0.2605	0.1930	4.0358	1.462	0.398	0.177	-2.57	0.24	
25	21.2862	0.3835	0.3411	0.3119	4.0705	1.710	5.930	0.136	-1.82	0.18	*
27	20.9620	0.4201	0.3533	0.0944	3.9173	2.328	0.985	0.156	-2.09	0.21	
28	21.1103	0.4367	0.3305	0.1880	3.9909	1.712	6.234	0.156	-2.18	0.21	*
29	21.0918	0.5195	0.6465	0.1672	3.4223	1.529	5.983	0.225	-2.12	0.30	
30	21.2023	0.3684	0.2356	0.1205	3.6366	2.060	0.933	0.183	-1.71	0.25	
32	21.0954	0.3225	0.3235	0.3422	3.9962	2.185	5.995	0.270	-1.09	0.36	
33	21.1307	0.3173	0.3863	0.1106	3.7809	1.359	6.199	0.155	-2.59	0.21	
34	21.2633	0.4045	0.2217	0.2377	4.2836	2.324	0.540	0.206	-0.86	0.28	
36	21.0509	0.3891	0.3177	0.2871	3.9562	1.524	5.890	0.100	-2.44	0.14	*
37	21.2053	0.3731	0.2829	0.1995	3.6804	1.418	5.892	0.155	-2.19	0.21	*
40	21.1469	0.3599	0.2782	0.1971	3.8310	1.481	6.267	0.176	-2.45	0.24	

Table 7—Continued

ID	A_0	R_{21}	R_{31}	R_{41}	ϕ_{21}	ϕ_{31}	ϕ_{41}	$\sigma_{\phi_{31}}$	[Fe/H]	$\sigma_{[Fe/H]}$	D_M pass? ^a
42	21.0392	0.3932	0.3089	0.1697	3.6708	1.710	6.045	0.150	-2.56	0.20	*
43	21.1188	0.3645	0.3324	0.2243	3.8744	1.791	6.075	0.151	-1.94	0.20	*
45	21.1690	0.4129	0.3552	0.2593	3.8733	1.391	5.584	0.133	-2.38	0.18	*
47	21.1743	0.3426	0.2996	0.1977	3.6999	1.895	6.150	0.178	-1.96	0.24	*
49	21.1237	0.3706	0.2392	0.1690	3.6302	1.731	5.878	0.196	-2.12	0.26	*
51	21.1322	0.3698	0.2734	0.1621	3.9393	1.626	5.700	0.161	-2.19	0.22	*
52	21.1344	0.5317	0.3492	0.0578	4.3725	2.834	1.716	0.122	-0.46	0.17	
53	21.0354	0.5495	0.3102	0.1556	4.0508	2.151	0.046	0.237	-1.65	0.32	
54	21.1544	0.4462	0.2972	0.2325	3.7941	2.109	0.717	0.221	-1.69	0.30	
55	21.0562	0.3807	0.2762	0.2315	3.9886	1.590	5.568	0.178	-2.21	0.24	*
56	21.1826	0.7219	0.7131	0.6050	4.0904	2.675	1.197	0.117	-0.64	0.16	
57	21.0546	0.4037	0.2996	0.1998	3.7945	1.673	6.110	0.203	-2.12	0.28	*
58	21.1601	0.4425	0.3006	0.1511	3.8126	2.012	6.026	0.299	-1.63	0.40	*
59	21.1954	0.3742	0.3120	0.1503	3.8208	1.539	5.581	0.111	-2.22	0.15	*
60	21.0932	0.3856	0.3667	0.0409	4.5573	2.133	1.630	0.292	-1.49	0.39	
62	21.1604	0.2769	0.2547	0.1082	3.6509	1.119	0.357	0.249	-2.89	0.34	
63	21.1308	0.4094	0.3034	0.1444	3.8708	1.520	0.566	0.239	-2.37	0.32	
64	21.1639	0.4044	0.2060	0.1087	3.5979	1.046	4.927	0.336	-2.97	0.46	
65	21.1341	0.4056	0.3401	0.1892	3.7348	1.263	5.416	0.196	-2.61	0.27	*
66	21.1917	0.4033	0.2293	0.1271	3.8670	1.352	1.749	0.227	-2.81	0.31	
69	21.1418	0.4391	0.3548	0.2247	3.8962	1.606	5.866	0.129	-2.15	0.18	*
70	21.0688	0.4295	0.3121	0.2121	3.6864	1.545	5.568	0.161	-2.41	0.22	*
74	21.1333	0.3436	0.3541	0.1874	3.8226	1.401	5.798	0.103	-2.43	0.14	
76	21.0668	0.5111	0.4381	0.3828	3.8159	1.663	5.946	0.135	-2.01	0.18	*
80	21.1615	0.4577	0.3232	0.2484	4.0232	1.726	5.872	0.195	-2.03	0.26	*
81	20.9603	0.4094	0.3117	0.1080	3.6554	2.259	2.538	0.239	-2.01	0.32	
82	21.1601	0.4776	0.2322	0.1698	3.8021	1.630	5.921	0.189	-2.11	0.26	*
84	21.0138	0.3621	0.2656	0.2341	3.9118	1.392	5.785	0.140	-2.44	0.19	
85	21.1101	0.3688	0.3734	0.1821	3.8898	1.411	5.390	0.175	-2.53	0.24	*
86	21.1539	0.4207	0.2335	0.0733	3.7654	1.913	6.089	0.337	-1.91	0.45	

Table 7—Continued

ID	A_0	R_{21}	R_{31}	R_{41}	ϕ_{21}	ϕ_{31}	ϕ_{41}	$\sigma_{\phi_{31}}$	[Fe/H]	$\sigma_{[Fe/H]}$	D_M pass? ^a
87	21.2338	0.3278	0.4763	0.1339	4.5433	2.335	1.365	0.200	-1.24	0.27	
88	21.1992	0.4304	0.3728	0.2675	3.6537	1.639	5.915	0.181	-2.15	0.25	*
89	21.1122	0.4373	0.2633	0.2134	3.9794	1.640	5.929	0.271	-2.18	0.37	*
92	21.2012	0.4593	0.2218	0.2490	4.0976	1.786	5.667	0.245	-1.73	0.33	
93	21.1188	0.3776	0.3039	0.2448	4.0668	1.558	5.937	0.132	-2.17	0.18	*
94	21.1455	0.4514	0.2628	0.2586	3.7857	1.543	6.005	0.125	-2.05	0.17	
95	21.0371	0.3973	0.2391	0.1905	3.8537	1.621	5.608	0.176	-2.26	0.24	*
98	21.0444	0.4845	0.3347	0.1981	3.8040	1.665	0.389	0.189	-2.26	0.26	
100	20.9654	0.3373	0.1896	0.0863	4.1915	1.908	1.242	0.299	-2.57	0.40	
101	21.1938	0.3419	0.4871	0.3298	3.9467	1.824	5.786	0.151	-1.99	0.20	*
102	21.0912	0.3846	0.1889	0.2116	3.5606	1.948	0.430	0.187	-1.60	0.25	
103	21.1933	0.4730	0.3462	0.2441	3.8644	1.724	5.684	0.177	-2.05	0.24	*
104	21.1413	0.3145	0.3785	0.2147	3.9168	1.419	5.685	0.111	-2.40	0.16	*
105	21.2349	0.3906	0.3318	0.1716	3.8405	1.935	6.225	0.147	-1.79	0.20	*
107	21.1280	0.4623	0.3735	0.2258	3.5859	1.489	5.910	0.163	-2.24	0.22	*
114	20.8940	0.3156	0.1729	0.1486	3.9526	1.759	6.230	0.237	-2.23	0.32	*
115	21.0860	1.6991	1.7997	0.9826	2.0955	0.667	6.012	0.324	-3.47	0.44	
116	21.1802	2.2240	2.8269	0.6754	0.1569	1.101	4.885	3.001	-3.35	4.04	
119	21.1065	0.3107	0.2153	0.1698	4.1220	1.915	0.517	0.278	-2.11	0.38	
122	21.1773	0.3763	0.3510	0.1807	3.8666	1.947	0.367	0.369	-1.92	0.50	
124	21.1814	0.4343	0.2887	0.2845	3.7266	1.512	5.377	0.118	-2.07	0.16	
125	21.0576	0.3962	0.2374	0.1322	3.9208	1.807	0.055	0.143	-2.36	0.19	
126	21.1108	0.3502	0.3280	0.2460	3.6596	1.565	5.892	0.147	-2.20	0.20	*
127	21.1686	0.3964	0.2482	0.1976	3.9177	1.577	6.208	0.142	-2.59	0.20	
128	21.1830	0.3977	0.3906	0.2593	3.6900	1.872	5.872	0.172	-2.00	0.23	*
129	21.2547	0.3290	0.1382	0.2019	4.1716	1.255	5.564	0.417	-2.62	0.56	
132	21.0987	0.1121	0.3401	0.1890	3.5035	2.589	6.112	0.166	-0.98	0.23	
133	21.0932	0.4467	0.2818	0.1231	3.8670	1.863	0.030	0.196	-1.88	0.26	
135	21.0948	0.4023	0.3453	0.1891	3.8332	1.757	5.891	0.117	-2.15	0.16	*
136	21.1900	0.3180	0.2411	0.2928	3.9378	1.784	5.756	0.424	-1.68	0.57	

Table 7—Continued

ID	A_0	R_{21}	R_{31}	R_{41}	ϕ_{21}	ϕ_{31}	ϕ_{41}	$\sigma_{\phi_{31}}$	[Fe/H]	$\sigma_{[Fe/H]}$	D_M pass? ^a
137	21.2138	0.3758	0.2625	0.1822	3.9266	1.589	5.710	0.168	-2.22	0.23	*
140	21.0901	0.2879	0.1967	0.2204	2.3131	1.191	4.132	1.184	-2.92	1.59	
142	21.0906	0.4665	0.3385	0.2569	3.7860	1.634	5.772	0.102	-2.36	0.14	*
144	21.3136	0.8180	0.2715	0.5360	2.4477	2.581	3.875	0.333	-0.74	0.45	
149	21.2231	0.3700	0.1774	0.1194	3.9287	3.235	0.367	0.394	-0.31	0.54	
150	21.0500	0.2377	0.1382	0.1382	4.3527	2.121	5.571	0.726	-1.89	0.98	
151	21.1498	0.3626	0.3154	0.0990	3.9220	1.622	0.008	0.209	-2.28	0.28	
152	21.1560	0.3985	0.3967	0.2306	3.6581	1.786	6.260	0.119	-2.08	0.16	*
154	21.0598	0.3671	0.3369	0.1177	3.8109	1.313	5.592	0.158	-2.78	0.22	*
159	21.0791	0.4384	0.2648	0.2246	4.0971	1.953	6.277	0.135	-1.99	0.18	*
161	21.2265	0.3989	0.3224	0.2057	3.7740	1.729	6.173	0.143	-2.13	0.19	*
162	21.1348	0.4299	0.2925	0.1395	3.9167	1.702	5.922	0.162	-2.17	0.22	*
163	21.2684	0.4072	0.3391	0.2046	4.0556	2.067	6.148	0.314	-1.31	0.42	*
164	21.1045	0.3637	0.3045	0.2021	3.6531	1.378	5.967	0.316	-2.64	0.43	*
167	21.1274	0.3788	0.2584	0.2988	3.9965	1.796	0.072	0.203	-2.30	0.28	
171	21.1111	0.4379	0.2636	0.1877	3.8213	2.009	6.264	0.255	-1.61	0.34	*
172	20.9743	0.3988	0.3147	0.1148	3.7654	1.898	0.471	0.124	-2.13	0.17	
174	20.9688	0.5443	0.2898	0.2588	4.2496	2.078	6.195	0.163	-1.95	0.22	*
175	21.1595	0.4584	0.2483	0.1598	3.8483	1.593	5.813	0.151	-1.99	0.20	*
176	20.7044	0.4697	0.2381	0.1348	3.7171	1.321	5.613	0.214	-2.60	0.29	*
177	21.0706	0.9609	0.5962	0.8721	5.1753	5.931	0.622	0.377	3.97	0.56	
178	21.1075	0.3318	0.3033	0.2832	3.8723	1.613	0.042	0.133	-2.14	0.18	
180	21.0667	0.4906	0.3366	0.1060	3.9508	2.642	1.553	0.367	-1.06	0.50	
183	21.1632	0.4588	0.3604	0.2331	3.7826	1.490	5.939	0.153	-2.32	0.21	*
185	21.2703	0.4016	0.2601	0.1861	3.8097	1.540	5.831	0.242	-2.24	0.33	*
187	21.1778	0.6475	0.4987	0.3929	2.0980	2.169	3.850	0.154	-1.89	0.21	
196	21.2136	0.4445	0.3840	0.1823	3.8577	1.506	5.976	0.137	-2.27	0.19	*
198	21.0808	0.3530	0.2225	0.0692	3.6715	1.804	1.183	0.255	-2.35	0.34	
199	21.1064	0.4746	0.3464	0.1720	4.0304	2.074	0.341	0.148	-1.90	0.20	
201	21.1134	0.3684	0.4381	0.2510	4.2339	1.746	0.049	0.216	-2.32	0.29	

Table 7—Continued

ID	A_0	R_{21}	R_{31}	R_{41}	ϕ_{21}	ϕ_{31}	ϕ_{41}	$\sigma_{\phi_{31}}$	[Fe/H]	$\sigma_{[Fe/H]}$	D_M pass? ^a
207	21.1579	0.3866	0.3150	0.2058	3.6818	1.372	5.550	0.217	-2.33	0.29	*
213	21.1666	0.4452	0.2605	0.1771	3.9542	2.009	5.510	0.276	-1.75	0.37	
216	21.1330	0.4461	0.3912	0.2201	3.3530	1.542	6.217	0.105	-2.24	0.14	
218	21.1418	0.4827	0.3112	0.2325	3.8122	1.236	4.587	0.253	-2.75	0.34	
219	21.2374	0.4351	0.3167	0.1716	3.9298	1.522	5.540	0.164	-2.33	0.22	*
220	21.1473	0.4628	0.2067	0.1128	3.5244	1.388	5.629	0.286	-2.62	0.39	*
223	21.2273	0.3467	0.3532	0.1648	3.9499	1.824	0.257	0.109	-1.89	0.15	
225	21.1668	0.3397	0.3088	0.1798	3.8777	1.429	5.352	0.268	-2.30	0.36	*
227	21.1436	0.4977	0.4236	0.2166	4.1281	1.515	0.083	0.167	-2.32	0.23	
237	21.2335	0.4387	0.3462	0.1824	3.8619	1.578	5.537	0.127	-2.30	0.17	*
238	21.0892	0.3513	0.2782	0.1435	3.6480	1.495	5.621	0.130	-2.13	0.18	*
243	21.0025	0.2285	0.1968	0.1412	4.1500	2.210	1.336	0.314	-2.02	0.42	
244	21.2050	0.2709	0.1472	0.1502	3.9090	1.318	5.572	0.206	-2.37	0.28	*
249	21.1367	0.3947	0.3224	0.2133	3.8850	1.689	5.687	0.086	-2.07	0.12	*
252	21.1382	0.4386	0.3597	0.2268	3.8585	1.453	5.479	0.133	-2.30	0.18	*
253	21.2784	0.2496	0.1984	0.5095	4.7083	4.776	4.581	0.357	2.34	0.51	
258	21.0697	0.3559	0.3024	0.1948	3.7039	1.365	5.571	0.124	-2.45	0.17	*
260	21.1105	0.5214	0.3487	0.2697	3.9380	1.576	5.989	0.085	-1.98	0.12	
261	21.1359	0.4000	0.2921	0.1263	3.7906	1.831	0.182	0.167	-1.62	0.22	
262	21.1091	0.3866	0.3278	0.1781	3.5986	1.408	6.122	0.092	-2.56	0.13	
265	21.0829	0.4074	0.2783	0.2220	3.7921	1.488	5.868	0.403	-2.26	0.54	*
269	21.0926	0.4347	0.3432	0.2381	3.7428	1.413	5.332	0.127	-2.14	0.17	*
270	20.9785	0.3460	0.3707	0.2696	3.7410	1.306	5.605	0.085	-2.41	0.12	*
273	20.9756	0.0759	0.0814	0.1433	5.2331	2.817	1.126	0.859	-1.55	1.16	
278	21.1312	0.3491	0.3719	0.2490	3.7717	1.668	5.850	0.143	-2.20	0.19	*
279	21.0067	0.4360	0.2030	0.1760	3.6151	1.206	5.978	0.223	-2.79	0.31	
281	20.8779	0.2710	0.6362	0.3831	1.8806	4.044	0.350	0.089	0.70	0.17	
284	21.0144	0.1990	0.3959	0.2275	4.0643	1.113	5.740	0.228	-2.92	0.31	
285	20.8499	0.3775	0.2681	0.1193	4.1360	1.897	0.200	0.281	-2.06	0.38	
290	21.1048	0.4284	0.1804	0.1608	3.8519	1.824	1.108	0.491	-2.48	0.66	

Table 7—Continued

ID	A_0	R_{21}	R_{31}	R_{41}	ϕ_{21}	ϕ_{31}	ϕ_{41}	$\sigma_{\phi_{31}}$	[Fe/H]	$\sigma_{[Fe/H]}$	D_M pass? ^a
291	20.7762	0.7227	0.5494	0.4493	3.8448	1.340	4.926	0.102	-3.28	0.15	
298	21.1788	0.3668	0.2674	0.2986	3.8061	0.882	4.773	0.257	-3.42	0.35	
303	21.2060	0.3931	0.3419	0.1996	4.3250	2.005	0.412	0.102	-1.74	0.14	
304	21.1033	0.4119	0.2785	0.1459	3.9121	1.802	5.678	0.234	-2.27	0.32	*
308	21.0490	0.3422	0.0718	0.2947	3.0191	0.890	4.789	0.953	-3.24	1.28	
309	21.0466	0.3957	0.2182	0.2359	3.2974	1.333	5.126	0.208	-2.68	0.28	
310	21.0316	0.4385	0.3614	0.3383	4.1751	2.114	0.496	0.170	-1.74	0.23	
313	21.0945	0.3778	0.2171	0.1559	3.8761	1.283	4.963	0.184	-2.48	0.25	*
315	21.0593	0.4135	0.1561	0.1555	3.5577	1.364	0.402	0.316	-2.41	0.43	
323	21.0327	0.3434	0.2483	0.2011	3.9195	1.239	5.380	0.153	-2.45	0.21	*
324	21.0505	0.4123	0.2956	0.1909	3.7772	1.367	5.935	0.132	-2.52	0.18	
325	21.0045	0.2638	0.3611	0.1385	4.5856	2.350	0.748	0.269	-1.27	0.36	
326	21.0456	0.4710	0.2458	0.2248	3.4030	1.104	5.710	0.160	-3.02	0.22	
332	21.1832	0.2445	0.3541	0.4182	3.7120	0.430	5.168	0.443	-3.91	0.60	

^aStars with an * have passed the $D_M < 5.0$ criterion.

Table 8. Table of parameters for Draco anomalous Cepheids.

ID ^a	RA (2000.0)	DEC (2000.0)	Period (days)	Amp	$\langle V \rangle$	$\langle I \rangle$	M_V
31	17:20:25.15	57:52:53.3	0.61763	0.71	19.57	18.78	-0.01
134*	17:19:06.37	57:49:48.2	0.59228	0.85	18.78	18.40	-0.80
141*	17:20:17.82	57:57:07.8	0.90087	0.67	19.20	18.63	-0.38
157*	17:19:08.08	57:58:35.2	0.93649	1.04	18.85	18.41	-0.74
194*	17:19:36.06	57:54:15.6	1.59027	0.48	18.11	17.53	-1.47
204*	17:22:00.74	57:50:21.2	0.45413	0.75	19.23	18.77	-0.35
230	17:21:47.77	57:53:18.9	0.60816	0.38	19.25	18.54	-0.33
282	17:19:42.55	57:54:49.8	0.55187	0.60	19.51	18.90	-0.05
312	17:18:30.56	57:56:04.8	0.90735	0.90	19.15	18.59	-0.43

^aStars denoted with an asterisk are previously known anomalous Cepheids (Norris & Zinn 1975; Zinn & Searle 1976; Nemec et al. 1988a)

Table 9. Long period, semi-irregular red variable stars and carbon stars.

ID	RA (2000.0)	DEC (2000.0)	V	I	$V - I$	σ_V	σ_I	Comment
302	17:18:52.12	58:04:13.2	17.26	15.88	1.38	0.04	0.03	1
293	17:19:10.82	57:59:17.7	17.14	15.76	1.39	0.03	0.01	1
292	17:19:17.52	58:01:07.4	16.84	15.35	1.48	0.06	0.03	1,2 var.vel.
288	17:19:42.39	57:58:38.0	17.25	15.99	1.26	0.07	0.08	1 carbon star (C5)
283	17:19:57.66	57:50:05.7	17.15	15.66	1.49	0.08	0.04	1,2 carbon star (C1), var.vel.
280	17:20:00.70	57:53:46.8	17.30	15.99	1.31	0.05	0.04	1,2,3 carbon star (C2)
274	17:20:32.85	57:51:44.2	16.91	15.38	1.53	0.06	0.05	1,2,3
272	17:20:40.26	57:57:33.1	16.44	14.90	1.55	0.02	0.02	1,3
271	17:20:41.85	58:00:25.1	16.93	15.44	1.48	0.05	0.02	1,2
268	17:20:43.69	57:48:44.3	16.51	15.03	1.48	0.04	0.03	1,2 var.vel
263	17:20:53.01	57:55:58.0	17.23	15.70	1.53	0.02	0.02	1,2,3
259	17:21:02.23	58:15:38.7	17.15	15.75	1.41	0.04	0.03	1
	Eclipsing binaries							
296	17:19:06.16	57:41:21.1	19.54	18.16	1.38	0.15	0.12	P=0.2435d
256	17:21:18.30	58:14:29.9	18.54	17.28	1.26	0.03	0.10	P=0.1253d or 0.2300d

References. — 1 = Draco RV member (Armandroff et al. 1995); 2 = Draco RV member (Olszewski et al. 1995); 3 = Draco proper motion member (Stetson 1980)

Table 10. QSOs found in our Draco survey. The last column lists where the spectra, if available, were obtained.

ID	RA (2000.0)	DEC (2000.0)	V	I	$V - I$	σ_V	σ_I	Comment
331	17:17:35.09	57:56:26.2	19.66	18.98	0.67	0.07	0.06	WIYN
329	17:17:50.11	58:11:08.1	19.96	19.13	0.83	0.08	0.06	probable QSO
328	17:17:50.57	58:15:14.7	17.71	16.92	0.79	0.06	0.06	SDSS
322	17:18:09.35	58:07:16.3	19.86	19.44	0.42	0.07	0.07	WIYN
320	17:18:19.40	57:39:35.2	20.18	19.30	0.87	0.15	0.06	WIYN
311	17:18:31.90	58:08:44.3	19.17	18.85	0.32	0.14	0.04	WIYN
300	17:19:01.71	58:00:29.1	19.31	18.60	0.71	0.06	0.02	WIYN, SDSS
299	17:19:04.18	58:03:29.4	20.36	19.88	0.48	0.11	0.07	WIYN
203	17:19:34.43	57:58:49.8	19.51	18.80	0.71	0.20	0.10	WIYN ^a
287	17:19:43.77	58:11:12.4	19.87	18.85	1.01	0.06	0.04	SDSS
266	17:20:51.96	57:41:59.9	19.52	18.99	0.53	0.07	0.04	probable QSO
264	17:20:52.31	57:55:13.4	19.86	19.43	0.40	0.08	0.06	WIYN
257	17:21:18.12	57:33:30.5	20.25	19.19	1.05	0.17	0.08	probable QSO
255	17:21:22.85	57:50:29.5	17.90	17.26	0.64	0.02	0.01	WIYN, SDSS
254	17:21:25.49	58:15:28.2	20.34	19.65	0.69	0.08	0.05	SDSS
251	17:21:30.06	57:40:15.8	19.69	19.15	0.54	0.06	0.05	WIYN
240	17:21:41.47	57:52:35.6	20.65	19.83	0.82	0.09	0.08	probable QSO
241	17:21:41.57	57:33:18.9	18.88	18.24	0.64	0.06	0.17	WIYN, SDSS
231	17:21:47.52	58:15:07.8	19.96	18.46	1.50	0.14	0.04	WIYN
229	17:21:48.30	57:58:05.8	20.70	19.75	0.95	0.11	0.07	SDSS
224	17:22:07.34	58:14:25.0	20.79	20.25	0.54	0.25	0.14	probable QSO
222	17:22:11.66	57:56:52.2	20.74	19.77	0.98	0.16	0.09	WIYN, SDSS
215	17:22:36.06	57:37:05.0	20.10	19.90	0.21	0.19	0.08	WIYN
214	17:22:41.04	57:45:27.1	20.78	19.94	0.83	0.10	0.07	probable QSO
212	17:22:44.68	57:41:24.2	20.40	19.47	0.93	0.15	0.08	probable QSO
211	17:22:51.01	57:41:18.5	19.80	19.27	0.53	0.14	0.06	WIYN
210	17:22:56.95	58:11:10.8	19.76	19.01	0.75	0.14	0.08	WIYN, SDSS
209	17:23:01.83	58:04:06.7	20.52	19.10	1.42	0.14	0.07	probably QSO ^b
208	17:23:02.20	58:04:14.5	20.17	19.45	0.71	0.08	0.06	WIYN
206	17:23:14.18	58:14:07.4	19.99	19.57	0.42	0.17	0.09	WIYN

Table 10—Continued

ID	RA	DEC	V	I	$V - I$	σ_V	σ_I	Comment
	(2000.0)	(2000.0)						

^aB&S V203

^bonly 8'' from QSO at RA=17:23:02.20, DEC=+58:04:14.5.